OMV **AUSTRALIA PTY LTD**

ACN 082 932 027

SOLE DEVELOPMENT

(Patricia Baleen Extension)

Reservoir Simulation Study

SD-01-RE-0012

Part E

March 2004

Table of Contents

Figures

Tables

Appendices

1 EXECUTIVE SUMMARY

A reservoir simulation study of the Sole field was carried out to determine the range of reserves in the field. This was done by:

- Generating field and well production profiles for FEED studies and economic evaluation
- Determining the range of recovery factors over a range of subsurface uncertainties and development options

Upscaled geological models from Roxar modelling software (RMS) were exported into Eclipse reservoir simulation software. The P50 GIP model (base case simulation model) is based on the most likely structural map.

The base case simulation model assumes two conventional 7" wells located in the main lobe of the field. The simulation study also assumes a 14" pipeline to the existing Patricia Baleen onshore gas plant would export production from the Sole field and that the capacity of the plant is increased to accommodate 120 MMscf/d maximum plant throughput. Production profiles were generated assuming Sole production utilises the remaining capacity at the Patricia Baleen Plant.

The base case model simulation reserves is estimated at 227 Bcf with a recovery factor of 66%, based on the P50 GIP estimate of 346 Bcf. Field life is estimated at 8 years. It is assumed that Sole production commences 1st January 2005. The actual production date is primarily a function of a Gas Sales Agreement.

In the event that the start up date for Sole production is delayed, there may be a slight reduction in the expected field life of the Sole field under the base case model, with no change in reserves. This is a result of the potential for increased offtake from the Sole field due to the expected increased available plant capacity as a result of Patricia Baleen production decline. In the unlikely scenario that all of the onshore plant capacity is available to Sole over its field life, the Sole field life (P50) could be as short as 7 years.

Multiple reservoir simulation runs were conducted to establish the range of recoveries and production profiles from the Sole field. Sensitivities were run for a range of subsurface uncertainties. Key sensitivities investigated were:

- Residual gas
- Aquifer strength
- kv/kh
- Permeability distribution
- Reservoir barriers

The range of reserves for the P50 GIP model varied from 209 Bcf to 264 Bcf, based on the subsurface sensitivities investigated. Residual gas was identified as the key parameter influencing the recovery factor.

Sensitivities were also run for a range of development options:

- Well location & well number
- Well type & well size
- Pipeline size
- Onshore plant capacity

Simulation models were also developed for the P90 (300 Bcf) GIP model, based on the minimum case structural map (P90) and a P10 (398 Bcf) GIP model, based on the maximum case structural map (P10).

2 INTRODUCTION

The Sole field is located in Retention Lease VIC/RL3 in the offshore Gippsland Basin, Victoria. The field is approximately 35 km offshore and 65 km from the existing Patricia Baleen Gas Plant. The Sole-1 discovery well was drilled in 1973 by Shell Development Australia. The Sole-2 appraisal well was drilled in July 2002.

This reservoir simulation study was carried out to determine the range of reserves in the field, with the principal objectives of:

- Generating field and well production profiles for FEED studies and economic evaluation
- Determining the range of recovery factors over a range of subsurface uncertainties and development options

3 GEOLOGICAL MODELLING

3.1 3D Static Model

A 3D model was created from deterministic structural maps defined from seismic interpretation of the Top Latrobe and a fixed GWC (ref. Part C). The model was populated in Roxar modelling software (RMS) with petrophysical data from the Sole-1 and Sole-2 wells. Stochastic modelling was used to populate data between well control points (ref. Part D).

3.2 Upscaling

The geological model containing 426,126 cells was upscaled for simulation modelling using a 2 x 2 x 2 coarsening of the model. The simulation grid contains 40 x 30 x 46 cells (X x Y x Z) resulting in a total number of 55,200 cells. Grid dimensions are approximately 200m x 200m x 2m. Comparisons between the fine scale and upscaled models for permeability, porosity and gamma ray shows good correspondence between the models (Figure E1).

Figure E1 Comparison between Fine Sale and Upscaled Models

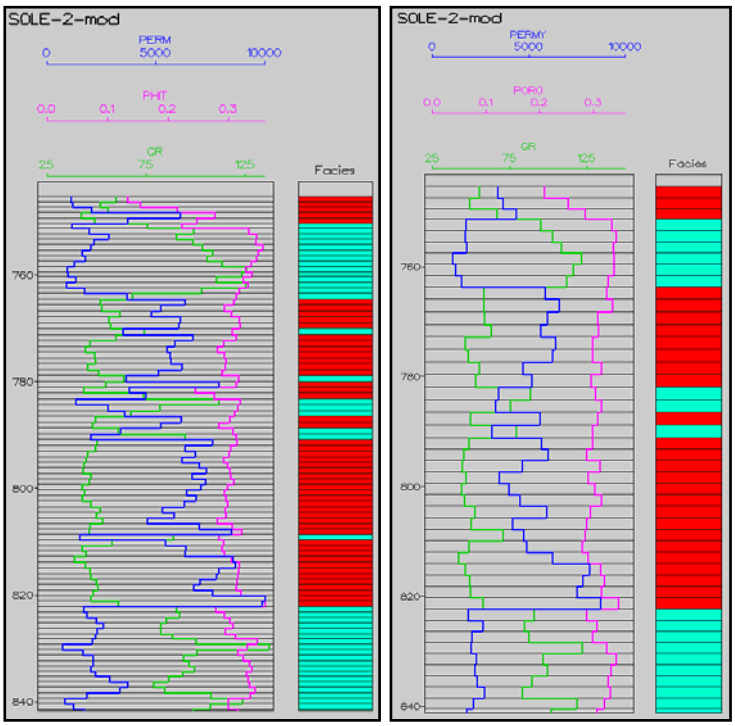

Porosity was upscaled for the simulation model using arithmetic averaging weighted by GRV. Permeability in the X and Y direction was upscaled using diagonal tensor while permeability in the Z direction was upscaled using diagonal tensor multiplied by 0.75, as per core measurements for kv/kh (ref. Part B). A comparison of the layer numbers in the geological model and the upscaled model is detailed in Table E1. Saturation was not upscaled from the geological model and is handled within Eclipse (see Section 4.4).

Table E1 Comparison of Geological and Simulation Models

Subgrid	Unit	Geological Model Layers	Simulation Model Layers
1	Latrobe Gp	1 - 6	1 - 3
2	LG_1	7 - 18	4 - 9
3	LG_2	19 - 43	10 - 21
4	LG_3	44 - 73	22 - 36
5	Top 20m of Kate Shale Eq.	74 - 93	37 - 46

3.3 Volumetrics

Gas-in-place (GIP) volumes were calculated for 10 realisations of the "most likely" structural model. The realisation closest to the mean GIP was used for the base case when upscaling and exporting to Eclipse (ref. Part D). A summary of the model is as follows:

- GRV = 496.0 MMm3
- GWC = 816.5 m
- Bg = 0.012 rcf/scf
- NTG = 100%
- GIP (Geological Model) = 358.5 Bcf
- GIP (Simulation Model) = 357.7 Bcf

4 DYNAMIC RESERVOIR MODEL

4.1 Reservoir Data

The following Reservoir Engineering data was available to initialise the model:

- 2 FIT pressure points in Sole-1 gas leg (1973)
- MDT pressure points in both the gas and water legs of Sole-2 (2002)
- Sole-2 Drill-stem Test (2002)

Figure E2 shows the results of the Sole-2 Drill-stem Test. The test yielded a qualitative indication of high permeability. Core data subsequently confirmed multi-Darcy rock. The results confirm high deliverability and minimal drawdown across the reservoir.

Figure E2 Sole-2 DST Test Overview

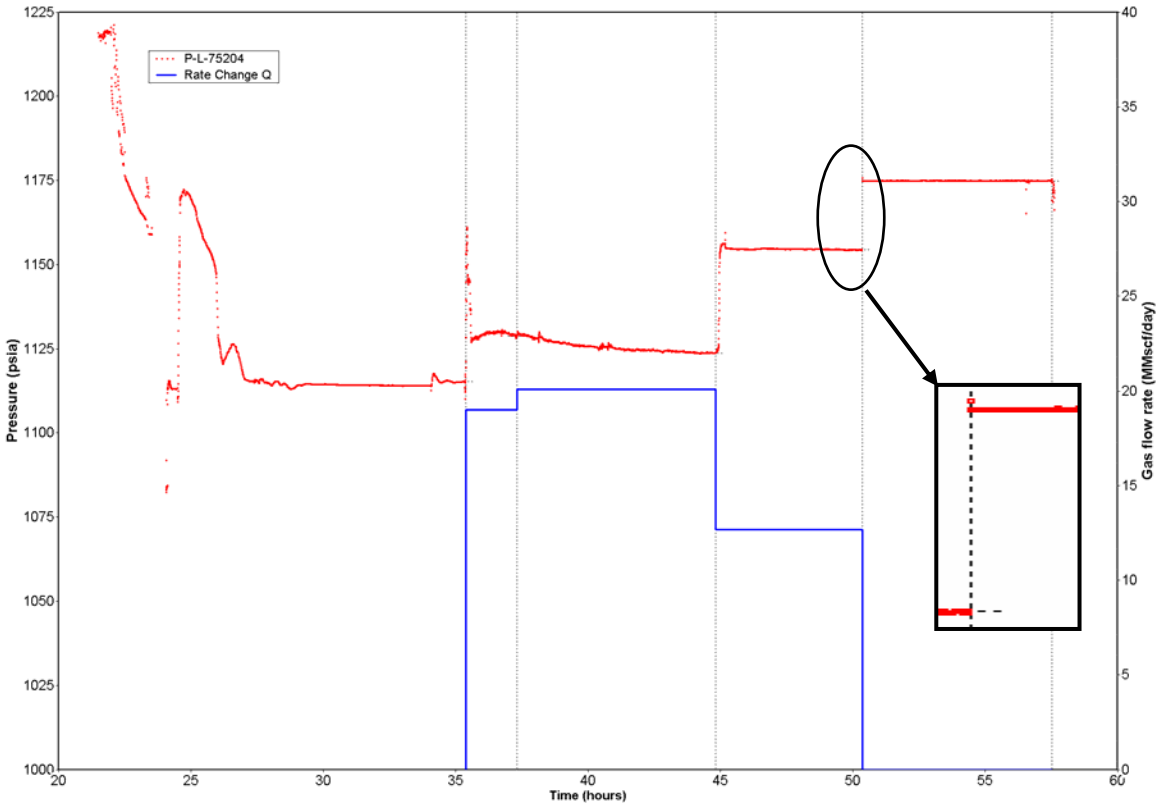

4.2 Model Initialisation

The Sole field reservoir simulation model was initialised with the following parameters:

Table E2 Model Initialisation Parameters

Reservoir Pressure	1180 psia
Reservoir Temperature	110 ^{o}F
Datum Depth (@ GWC)	816.5mSS

The FWL depth from Sole-2 MDT analysis was estimated at 816.6 mSS (Figure E3). Assuming a very small threshold entry pressure (insufficient resolution from capillary pressure tests), GWC depth was estimated at 816.5 mSS.

Average reservoir pressure was estimated at 1180 psia (at GWC of 816.5 mSS) from Sole-2 MDT wireline logs (2002). This was compared with bottomhole gauge data from the drill-stem test. The final gauge pressure of 1170.8 psia (1180.2 psia at datum depth) matched the formation pressure data obtained during wireline logging operations.

The Latrobe Reservoir in the Sole field has depleted approximately 45 psi since the drilling of Sole-1 (1973) to the drilling of Sole-2 (2002) (Figure E3). This is interpreted to be as a result of production from nearby fields that in turn deplete the massive Latrobe aquifer. This suggests that the reservoir is clearly in communication with the aquifer and supports the assumption of strong aquifer support. However this also assumes reservoir pressure is dropping at a rate of 1.5 psi/year. As a result there is a potential for reservoir pressure to drop some 4 - 5 psi before production commences.

If the reservoir is assumed to be filled to spill, then this drop in reservoir pressure could also result in a small loss of reserves, as a reduction in aquifer pressure will cause expansion of the gas contained within the Sole reservoir. The gas expansion factor (Eg) is also lowered.

Figure E3 Sole-2 MDT Data

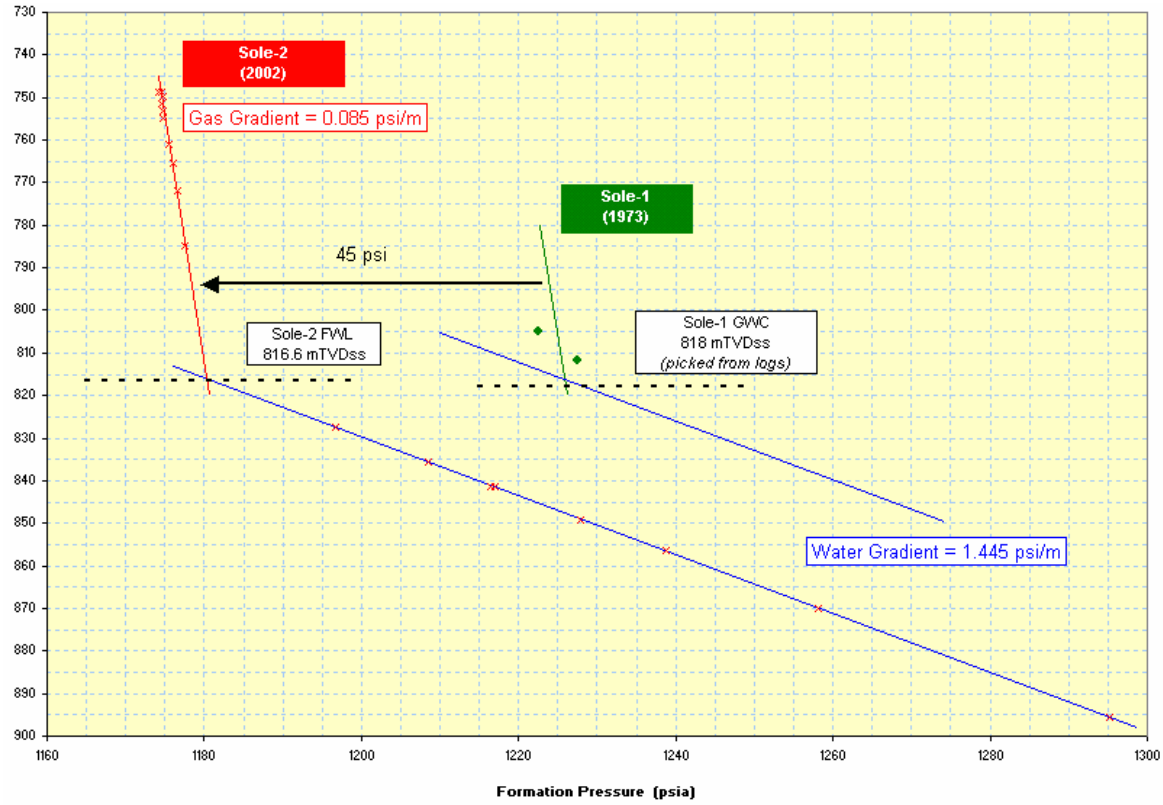

4.3 Fluid Properties

A total of six separator gas samples were recovered during Sole-2 drill-stem testing. A further two downhole gas samples were obtained using the wireline-conveyed MDT tool. The gas contained within the Sole reservoir comprises predominantly methane and is considered liquids free. All samples were analysed in the laboratory and were found to be in good agreement, with less than 1% variation in methane. The results for the 5th sample from DST have been used for analysis and are shown in Table E3.

Table E3 Sole Gas Composition

Component	CO_2	N_2	H_2S	C_1	C_2	C_3	iC_4	nC_4
mol %	1.12	3.23	0.11	94.16	1.21	0.14	0.02	0.01

The predicted heating value of Sole gas is 1.038 MJ/scf (@288.15°K). Based on current data from the Patricia Baleen plant, fuel and losses is estimated at less than 3%. As a result, scf and MJ have been used interchangeably in reservoir engineering work as gas produced (in MMscf/d) will be similar in magnitude to gas sold (in TJ/d). This assumption is conservative and remains valid if current fuel and losses increase by up to 40%. PVT tables were generated using the PVTi package from Geoquest. Table E4 is a summary of PVT data for an "averaged" gas composition.

Table E4 Sole PVT Properties

Gas Gravity	0.589	
Gas Heating Value (@15°C)	1.038	MJ/scf
	984	Btu/scf
At reservoir conditions:		
Gas Formation Volume Factor (Bg)	2.174	rb/Mscf
Gas Expansion Factor (Eg)	81.9	scf/rcf
Gas Viscosity	0.0135	cp

A most-likely Sole field H_2S concentration of 1,050 ppm has been determined following detailed compositional analysis of fluid samples recovered from the Sole-2 well (refer Appendix EA). A maximum H_2S concentration of 1500 ppm has been used for design purposes.

4.4 Capillary Pressure / Saturation Functions

Capillary pressure data from 12 core samples (Sole-2) was used to determine the saturation height function used in simulation. The analysis involved air-brine drainage capillary pressure measurements by porous–plate method. The capillary pressure curves for all 12 core samples are shown in Figure E4.

The high gamma sheetflood facies contained a far tighter range in permeability than the low gamma braided channel facies. The braided channel permeabilities were generally higher than the average permeability of the simulation model (~2900 md) and ranged from 1 – 10 Darcies. The sheetflood facies were generally clustered around 1 – 3 Darcies (see Part D). Excluding the data for k_{is} = 8106 md, a clear saturation versus permeability relationship exists.

A relationship for saturation-height modelling was derived using the Thomeer formula (Part B). The average permeability in the simulation model of ~2900 md was used to derive a single curve for population of the model. There is negligible difference for saturation versus height for varying facies.

As the capillary pressure curves were within a tight range of saturations for any given capillary pressure, there is little value expected from rigorous modelling of capillary pressure for different permeability ranges. For the permeabilities expected in the model, transition zones are sharp.

The GRV weighted average for initial gas saturation (above the GWC) in the simulation model is estimated at 79%.

Figure E4 Saturation Height Modelling Based on Sole-2 Core

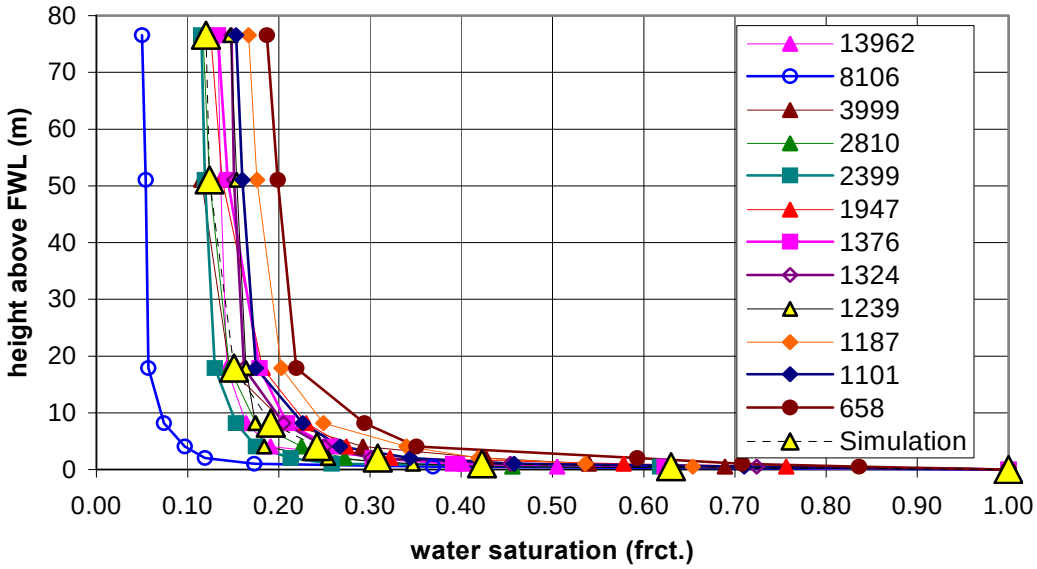

4.5 Residual Gas

A total of nine horizontal and four vertical core samples used for Sole-2 routine core analysis underwent residual gas measurements and subsequent water-gas relative permeability (end-point) by centrifuge. Further residual gas saturation (S_{gr}) measurements by counter current imbibition (CCI) were carried out on 4 selected samples that had previously undergone centrifuge S_{gr} measurements (water displacing gas). The same 4 samples then underwent S_{gr} measurements using decane instead of air.

The results of the air-brine centrifuge experiments are considered optimistic as the centrifuge can cause gas compression and as a result residual gas saturations are reduced (S_{gr} range 5 – 12%). CCI is considered pessimistic as water sweep through samples may be incomplete due to very low flowrates (S_{gr} range 23 – 29%). Decane-brine centrifuge experiments are considered optimal for determining S_{gr} as the incompressibility of decane avoids potential effects of compression that result with air-brine experiments (Sgr range 12 – 22%). An S_{gr} of 20% has been used in simulation. This could be considered conservative as 3 of 4 decane brine measurements were in the 12 – 15% range. Given the range of S_{gr} values measured, simulation model sensitivities were subsequently run for values of 10%, 15% and 25%.

4.6 Relative Permeability

Relative permeability curves were generated assuming Corey exponents of 2 for gas and 4 for water. Based on relative permeability end-point data, relative permeability to gas (k_{rg}) is estimated at 0.85 while relative permeability to water (k_{rw}) is estimated at 0.50. Initial water saturation (S_{wi}) is estimated at 12%, based on capillary pressure data. The relative permeability curves for a range of S_{gr} values are shown in Figure E5.

Figure E5 Relative Permeability Functions for Various Residual Gas Saturations

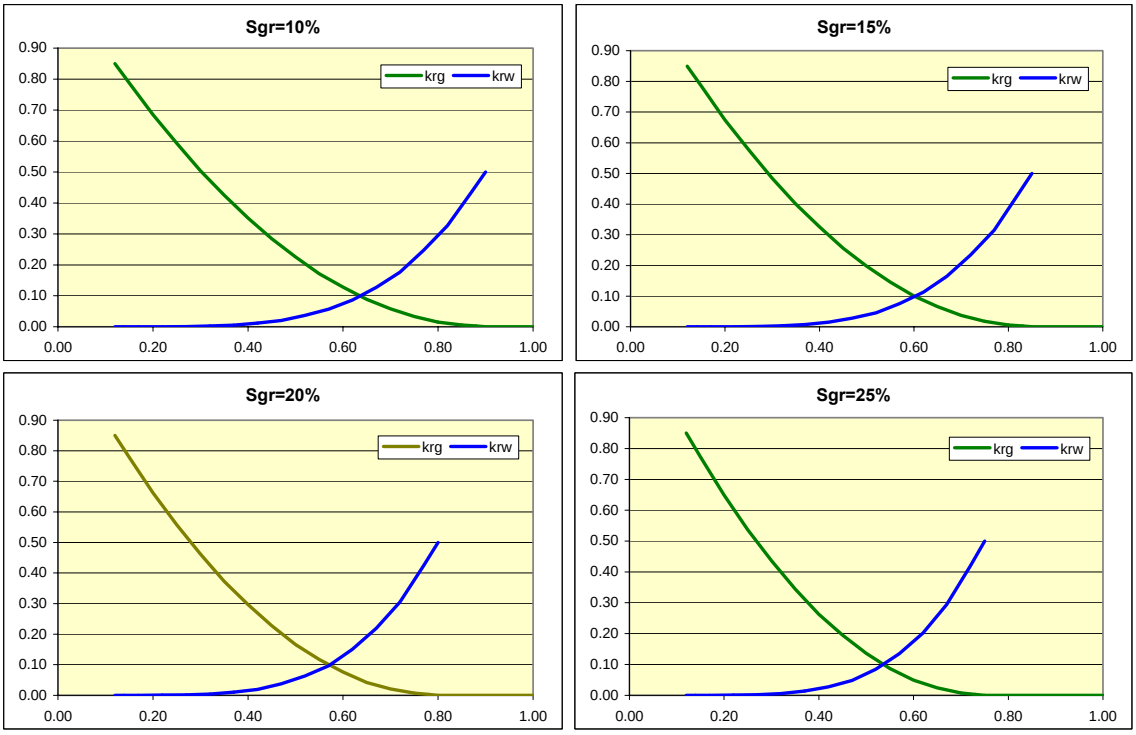

4.7 Reservoir Barriers

The central part of the field is crosscut by three normal faults striking NW-SE. These faults have a maximum throw of 3 to 17m. However as these faults have sand juxtaposed to sand, strong communication across the faults is expected. The high permeability sands throughout the reservoir are interpreted as allowing good lateral and vertical movement of fluids, with no significant barriers present. As part of the sensitivity analysis conducted during the reservoir simulation study, the effect of assigning zero transmissibility across these faults was investigated. The base case assumption was that all faults are fully transmissible.

4.8 Rock Compaction

Given the relatively small change in reservoir pressure and the resulting high rate of aquifer influx, rock compaction by means of pore volume reduction is considered negligible.

4.9 Aquifer properties

Reservoir quality is estimated to be in the Darcy range of permeabilities and strong aquifer support is expected in the Sole field.

The Latrobe Reservoir in the Sole field has depleted approximately 45 psi since the drilling of Sole-1 (1973) to the drilling of Sole-2 (2002) with no production from the Sole field. This is interpreted to be as a result of production from nearby fields that in turn

deplete the massive Latrobe aquifer. This suggests that the reservoir is clearly in communication with the aquifer and supports the assumption of strong aquifer support.

In the reservoir simulation model, an analytical aquifer is connected to the Eastern, Southern and Western portions of the Sole field. The northern bounding fault is expected to effectively shield the Sole field from significant aquifer influx from that direction. The base case assumption is that the aquifer is infinite. Aquifer properties were based on average reservoir data and analysis of the Sole-1 and Sole-2 logs (30% porosity, 1500 md permeability, 100 m thick at the edges and 20 m thick at the bottom).

4.10 Network Model, Tubing and Pipeline Flow Performance

The Eclipse “Network” option was used to model the flow from wellheads through the common subsea pipeline to the onshore processing facility.

The tubing and pipeline lift curves used in the simulation model were generated using the PROSPER software with the following base case assumptions:

- Sole-2 vertical well connected to a subsea wellhead and manifold
- Sole-3 vertical well connected to a subsea wellhead
- In-field flowline from Sole-3 wellhead to Sole-2 manifold
- Subsea flowline from Sole-2 manifold to onshore plan inlet valve

Plant arrival pressure is set at 300 psi (~2083 kPa) to maximise pipeline and compression capacity, and to avoid hydrate formation.

5 SIMULATION STUDY RESULTS

5.1 Simulation Case Summary

The following simulation models were exported from RMS to Eclipse:

- P50 model (GIP = 346 Bcf), based on the most likely structural map
- P50 model (GIP = 300 Bcf), based on the minimum case structural map (P90)
- P50 model (GIP = 398 Bcf), based on the maximum case structural map (P10)

A summary of all simulation cases is included in Appendix EB and EC. GIP numbers were based on estimated values from Probabilistic GIP work at the time simulation was being performed. Updated numbers are outlined in Part A. A full range of sensitivities was run on the P50 GIP model. For the P90 and P10 GIP models, sensitivities on the key parameter uncertainties of residual gas saturation and aquifer strength were investigated.

5.2 Base Case Model

The base case model assumes the following:

- Two vertical wells in the main lobe on the Sole field
- Wells are completed with 7” production tubing
- The Sole field utilises the existing Patricia Baleen (PB) Onshore Plant
- Sole production at 97% availability & 90% remaining capacity (after PB is considered)
- Sole production rates are constrained based on PB ACQ rates
- Plant throughput is 120 MMscf/d (including PB)
- Production from Sole-3 wellhead to Sole-2 manifold by 1.5 km subsea pipeline
- Infield subsea pipeline is 14” O.D.
- Production to shore is by 63.5 km subsea pipeline (14” O.D)
- Minimum Plant Inlet Pressure = 300 psi
- Maximum Field Water Production = 500 bwpd
- Minimum Economic Field Gas Rate = 5.0 MMscf/d

The following reservoir properties are assumed:

Table E5 Base Case Reservoir Properties

NTG	95	%
kv/kh	0.75	
S_{wi}	12	%
S_{gr}	20	%
k_{rg}	0.85	
k_{rw}	0.50	
k (average)	2900	md
Φ (average)	0.31	pu

The base case model simulation results are as follows:

- Reserves 227.1 Bcf
- Recovery factor 66%
- GIP 346 Bcf
- Field life 8 years

Gas is contained within three distinct regions in the model:

1. The “Main lobe” contains 81% of the GIP and is where Sole-2 was drilled
2. The “Sole-1 lobe” contains 9% of the GIP and is where Sole-1 was drilled
3. The “North lobe” contains 10% of the GIP

Recovery from each of these lobes is shown in Table E6.

Table E6 Base Case Region Analysis

Case		Total	FIP1 Main	FIP2 Sole-1	FIP3 North
base	GIP (Bcf)	346.0	278.7	31.4	35.9
	Recovery (Bcf)	227.1	209.4	13.5	4.2
	remaining (Bcf)	118.9	69.3	17.9	31.7
	outflow (Bcf)		-17.7	13.5	4.2
	RF	**66%**	**75%**	**43%**	**12%**

Maximum recovery efficiency can be estimated based on estimates for initial water saturation (S_{wi}) and residual gas saturation (S_{gr}). For S_{wi} = 12% and S_{gr} = 20%, a recovery efficiency of 77% could be achieved. Results from reservoir simulation show recovery efficiency from the main lobe is estimated at 75%. As a result, sweep efficiency in the main lobe is 97%. Recovery efficiency in the North and Sole-1 lobes is significantly less as the base case assumes no wells are drilled in these accumulations. However some outflow is expected from these lobes before upward movement of the GWC would effectively isolate these lobes from the main lobe.

Figure E6 shows the base case simulation grid design. The simulation grid contains 55,200 cells with approximate grid dimensions of 200 m x 200 m x 2 m. For simulation purposes, it was assumed that the existing Sole-2 location was used for a future 7" well and that a further well (Sole-3) is drilled to the northwest of Sole-2 with both wells accessing the main lobe.

Figure E6 Base Case Simulation Grid

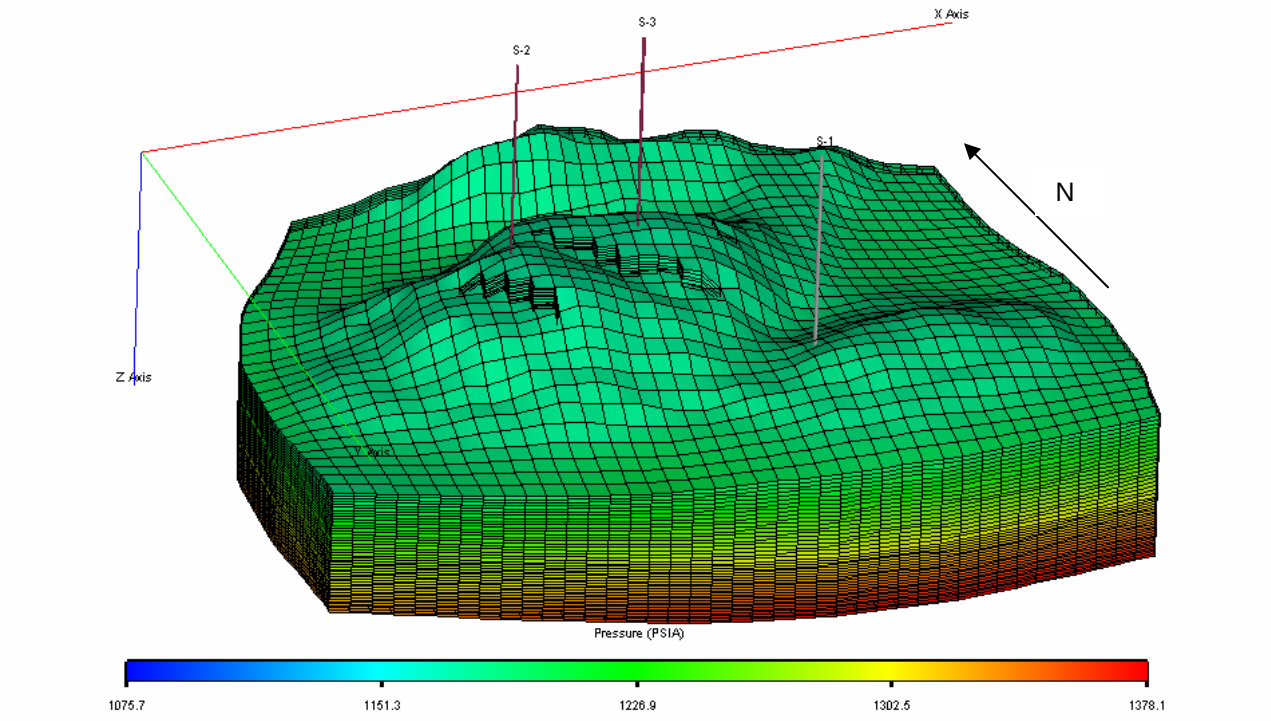

The expected gas and water rates for the base case model are shown in Table E7 and Figure E7. Cumulative gas production is also displayed. The production profiles show that production rates increase over time as the Patricia Baleen production declines. Production rates for Sole-2 and Sole-3 are expected to be very similar.

The current base case model predicts water to commence during the first quarter of 2011. Once water production begins, gas production is expected to decline quickly. In the simulation models, water production has been constrained to a maximum field rate of 500 bwpd. This is in line with planned water handling capacity onshore. The sensitivity of water production to the key subsurface uncertainties is summarised in sections to follow and with a Table summary in Appendix EB.

Table E7 Base Case Production Profiles

Year	**2005**	**2006**	**2007**	**2008**	**2009**	**2010**	**2011**	**2012**
Gas Prod. (Bcf)	29.3	32.0	33.5	34.9	35.8	36.3	23.1	2.2
Cum. Gas (Bcf)	29.3	61.4	94.8	129.7	165.4	201.8	224.9	227.1
Water Prod. (Mbbl)	0	0	0	0	0	0	106	122

Figure E7 Base Case Production Profiles

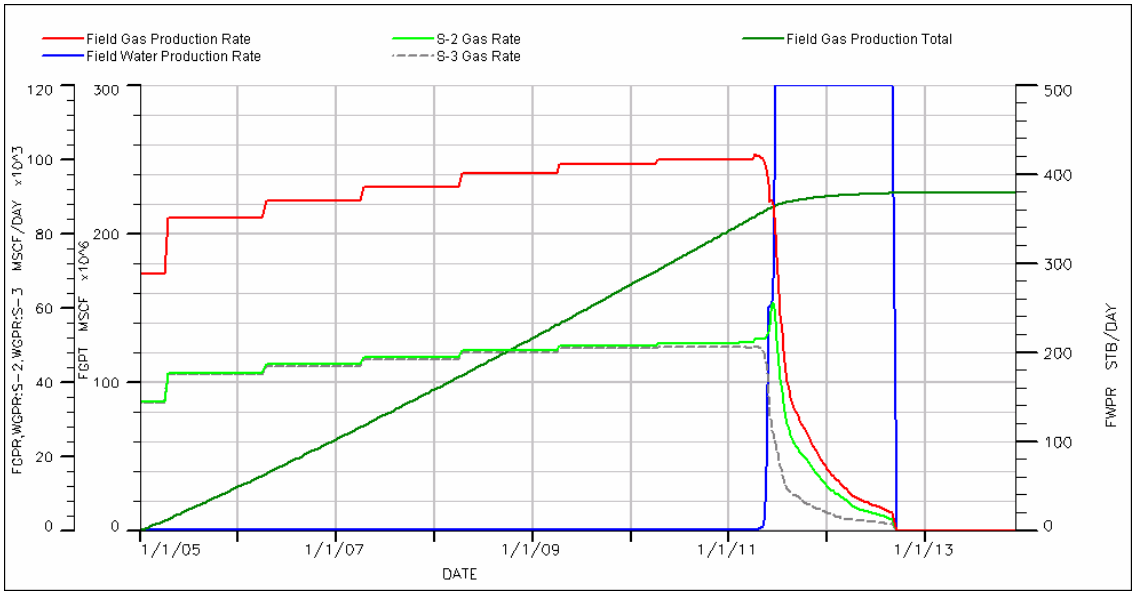

The expected tubing head and flowing bottomhole pressures expected for the individual wells are shown in Figure E8. Field pressure is also displayed. The pressure profiles show that average reservoir pressure never drops by more than 10% due to strong aquifer support. This is most evident at the end of field life, where production rates decline and average reservoir pressure rapidly increases.

Figure E8 Base Case Pressures

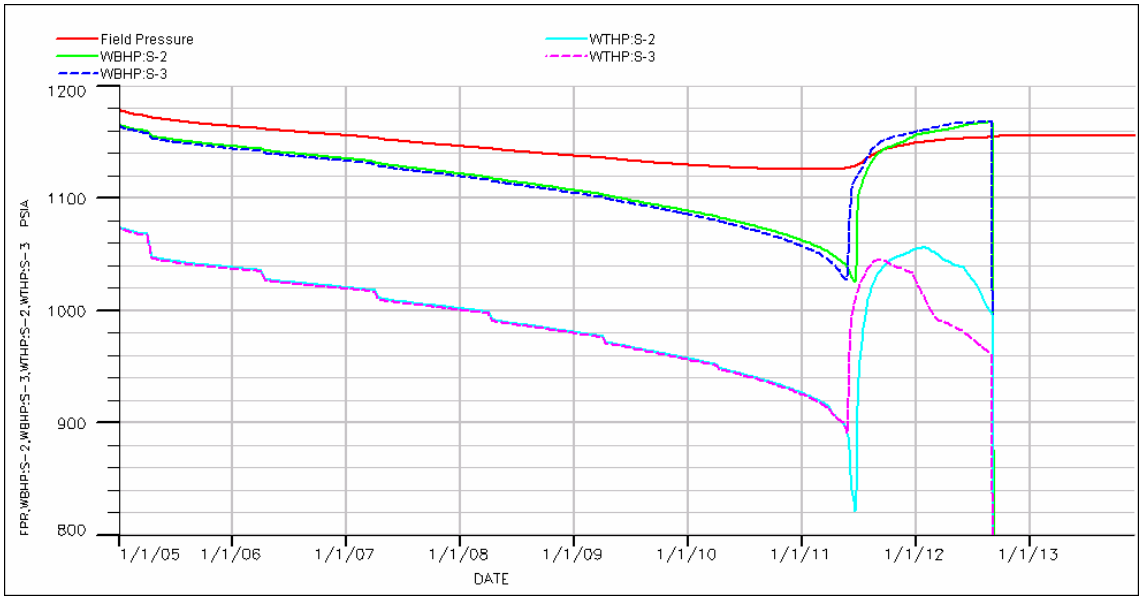

The gas saturation at the beginning and end of field life is shown in Figures E9 and E10. As highlighted in Table E6, gas recovery from the main lobe is close to expected maximum recovery efficiency, while some gas remains in the North and Sole-1 lobes.

Figure E9 Base Case Gas Saturation at Beginning of Field Life

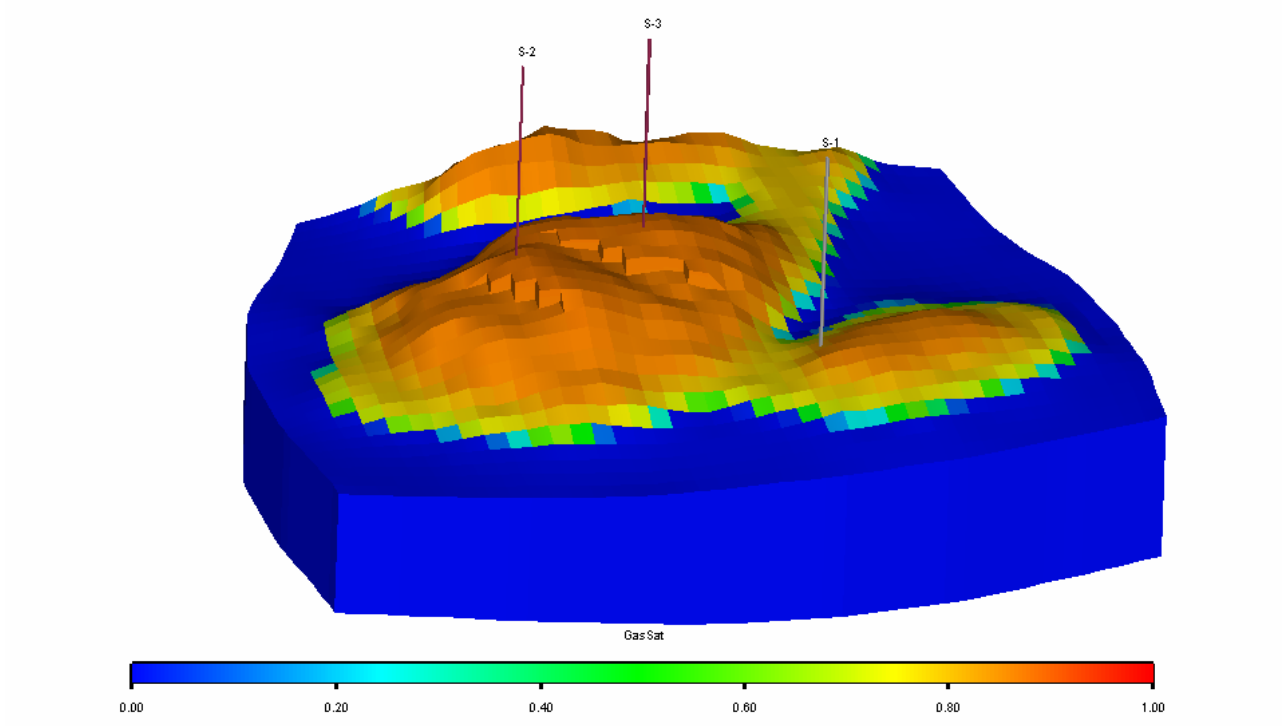

Figure E10 Base Case Gas Saturation at End of Field Life

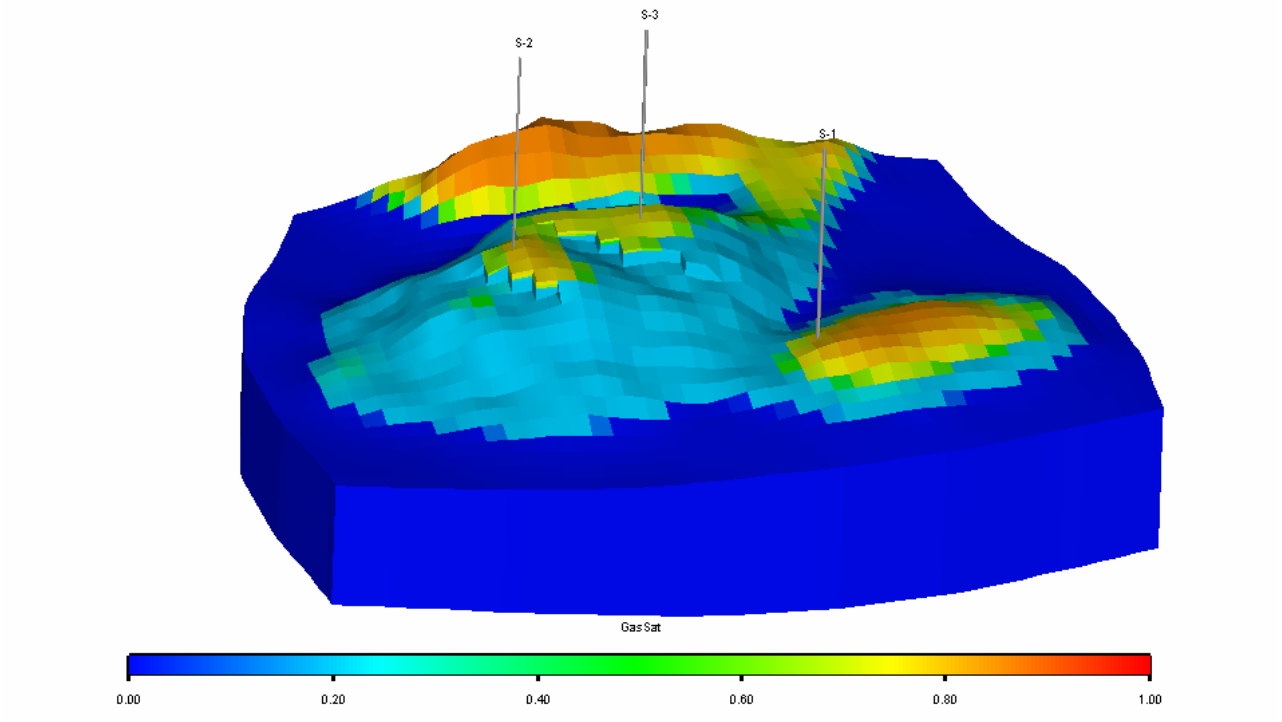

5.3 Sensitivities to Base Case Model

Sensitivities were run for a range of subsurface uncertainties and for a range of development options. The results are summarised in sections to follow.

5.3.1 Sensitivity to Residual Gas

The sensitivity of the base case to residual gas saturation was investigated in the following cases:

- Residual gas saturation at 10% (Case 201-sg10)
- Residual gas saturation at 15% (Case 201-sg15)
- Residual gas saturation at 25% (Case 201-sg25)

All cases were compared to the base case model where S_{gr} is modelled at 20%. The results are shown in Table E8.

Figure E11 shows Field Gas Production Rate (FGPR) vs. Date for all S_{gr} sensitivity cases, as well as Field Gas Production Total (FGPT) for all cases. The results show that any change to residual gas saturation has a significant impact on reserves. An absolute 5% increase or decrease in S_{gr} relates to an 8% change in reserves (or an absolute 5% change in recovery factor) at P50 reserves.

Table E8 Sensitivity to Residual Gas - Results

Case Summary	Case	GIP (Bcf)	Reserves (Bcf)	RF (%)
Base Case	base	346	227	66%
Residual gas saturation = 10%	201-sg10	346	264	76%
Residual gas saturation = 15%	201-sg15	346	245	71%
Residual gas saturation = 25%	201-sg25	346	209	60%

Figure E11 Gas Production Sensitivity to Residual Gas

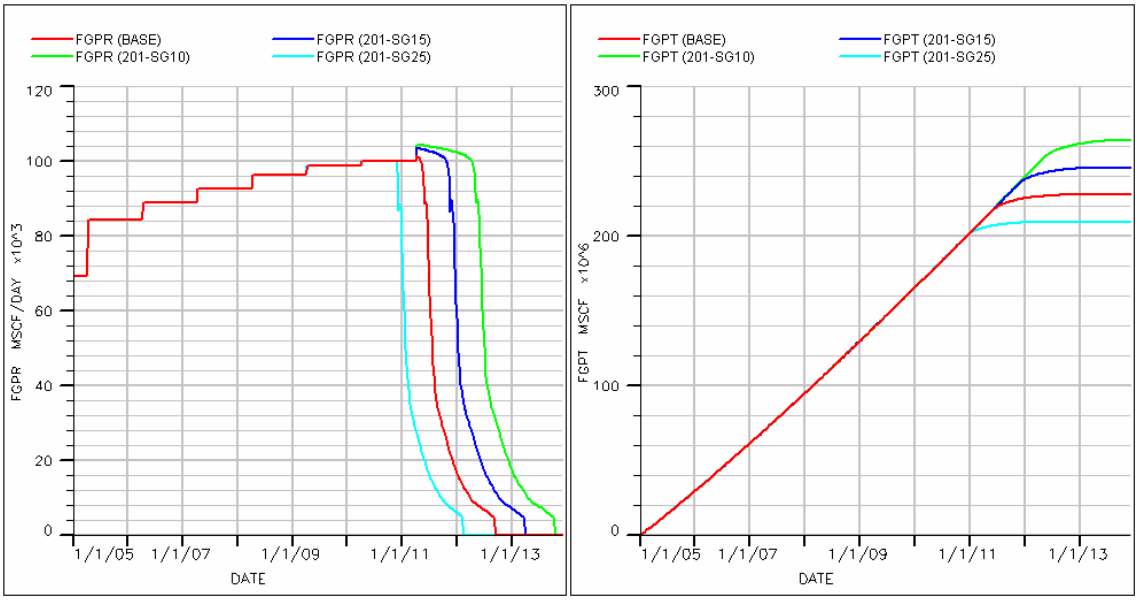

Figure E12 shows that water production commences earlier when the residual gas saturation is higher. This is expected as deliverability and the subsequent gas production rate is unchanged but recoverable gas volume is less, resulting in earlier water breakthrough.

Figure E12 Water Production Sensitivity to Residual Gas

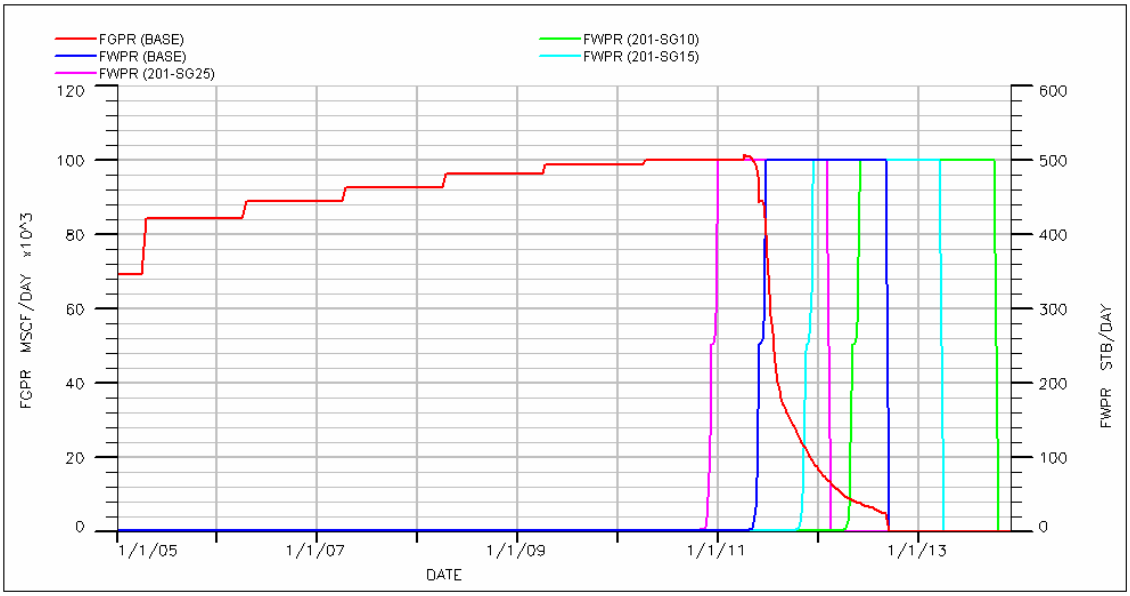

5.3.2 Sensitivity to Aquifer Strength

Sensitivities were run to determine the impact of different aquifer strengths and also to investigate the extreme case of no aquifer support.

The sensitivity of the base case to aquifer strength was investigated in the following cases:

- Low permeability aquifer: k = 100 md & no bottom-drive (Case 202-a100)
- High permeability aquifer: k = 3000 md (Case 202-a3000)
- No Aquifer (Case 202-noaq)

The results are shown in Table E9.

Table E9 Sensitivity to Aquifer Strength - Results

Case Summary	Case	GIP (Bcf)	Reserves (Bcf)	RF (%)
Base Case	base	346	227	66%
Aquifer: low perm. (100 md) & no bottom-drive	202-a100	346	233	67%
Aquifer: high perm. (3000 md)	202-a3000	346	226	65%
Aquifer: no aquifer	202-noaq	346	257	74%

Figure E13 shows recovery factor is relatively insensitive to permeability in the aquifer, with lower permeability providing the better recovery. However, if no aquifer support is assumed, recovery factor is increased significantly. This scenario is not expected to occur. One observation from the no aquifer case is that although recovery increases, time taken to reach end of field life is also increased and production rates are expected to drop much sooner than the cases where aquifer support is expected. In addition, reservoir pressures will drop much sooner. This will result in the need for additional gas compression requirements onshore.

Figure E13 Gas Production Sensitivity to Aquifer Strength

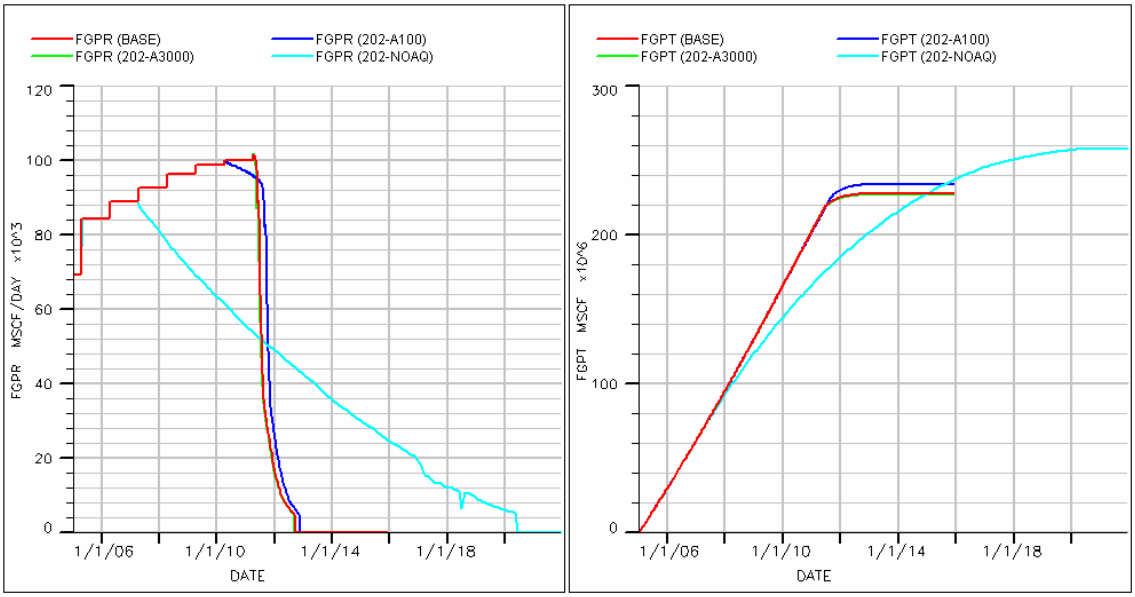

The pressure profiles are shown in Figure E14, highlighting the rapid decline in reservoir pressure for the no aquifer case.

Figure E14 Sensitivity to Aquifer Strength - Field Pressure Profile

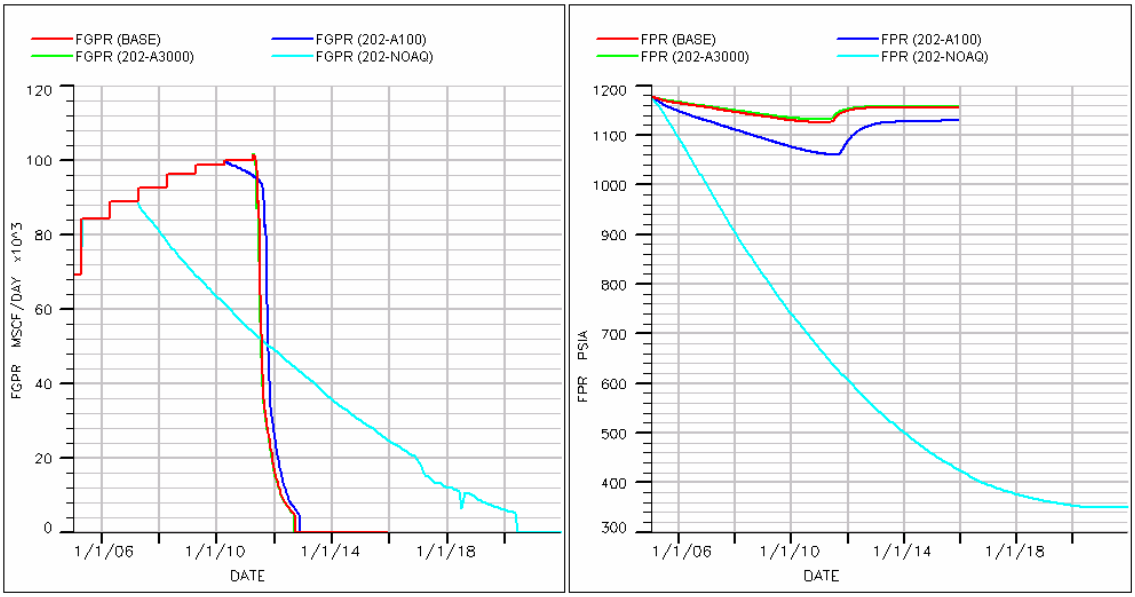

Figure E15 shows water production is relatively insensitive to permeability of the aquifer, with lower permeability in the aquifer delaying water production by 3 months.

Figure E15 Water Production Sensitivity to Aquifer Strength

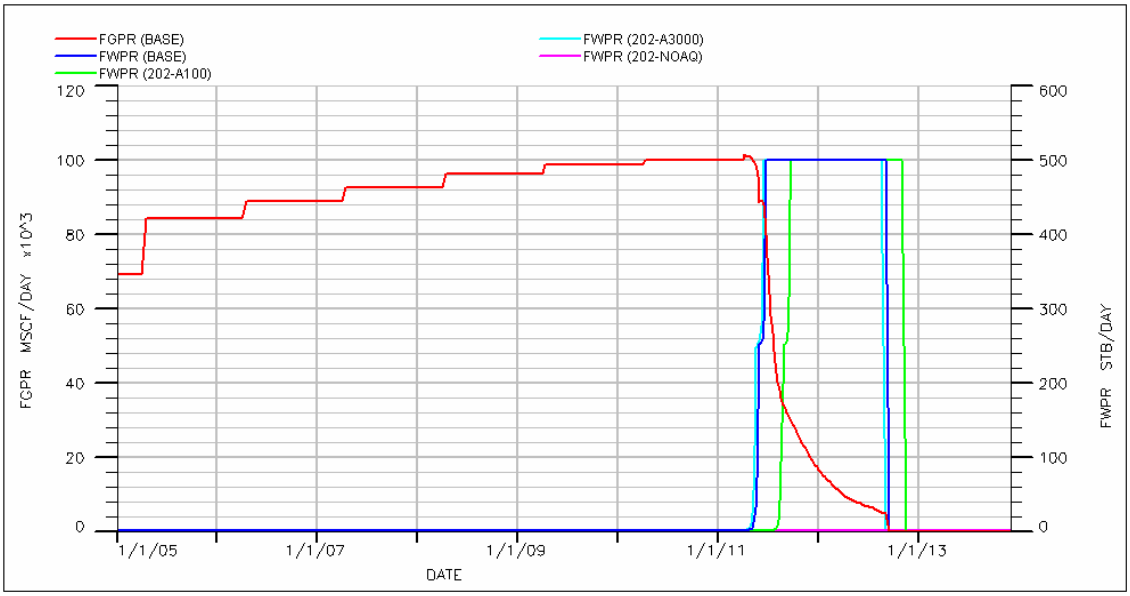

5.3.3 Sensitivity to Permeability

The sensitivity of the base case to vertical permeability and significant permeability changes was investigated in the following cases:

- Reduce kv/kh to 10% (Case 201-kv10)
- Increase kv/kh to 100% (Case 201-kv100)
- Permeability reduced by 50% across entire model (Case 201-reduce-k)
- Constant properties (pancake model) based on Sole-2 well (Case 201-pancake)

The results are shown in Table E10.

Table E10 Sensitivity to Permeability - Results

Case Summary	Case	GIP (Bcf)	Reserves (Bcf)	RF (%)
Base Case	base	346	227	66%
kv/kh = 10%	201-kv10	346	227	66%
kv/kh = 100%	201-kv100	346	227	66%
Permeability reduced by 50% across model	201-reduce-k	346	225	65%
Constant properties (pancake model) - S-2 well	201-pancake	346	231	67%

Figure E16 shows recovery factor is relatively insensitive to vertical permeability in the reservoir. A 50% reduction in permeability has little impact on reserves, suggesting permeability changes have little impact once reservoir permeabilities are in the Darcy range. The constant properties model slightly increased reserves. This result suggests stochastic modelling undertaken in Roxar has added some heterogeneity in permeability across the reservoir and therefore had a small impact in reducing reserves.

Figure E16 Gas Production Sensitivity to Permeability

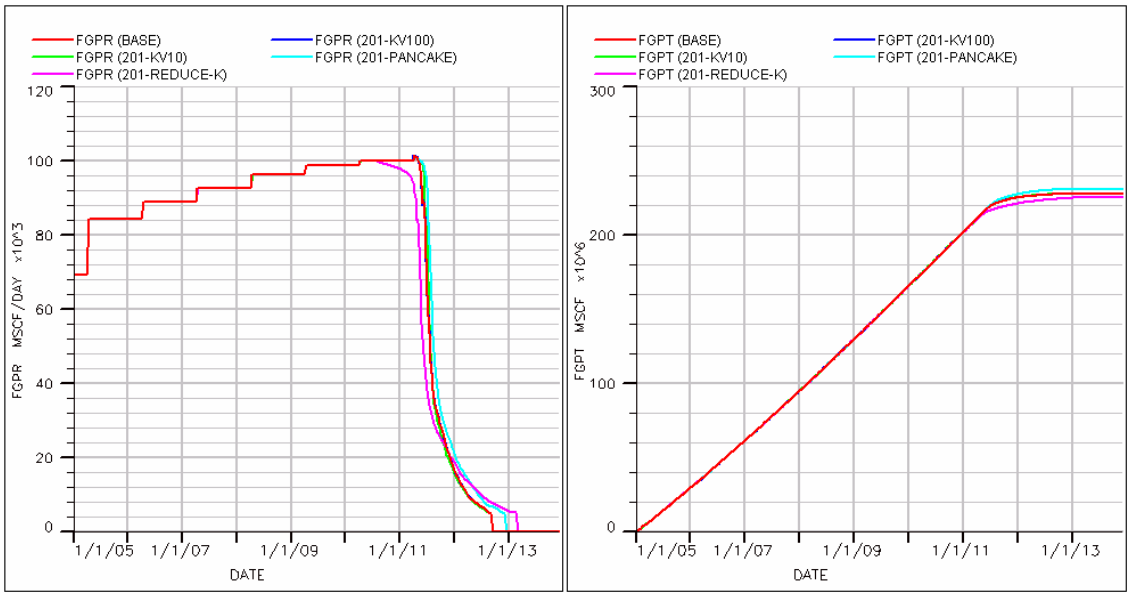

Vertical to horizontal permeability ratio and the impact of reduced permeability or assuming constant properties across the field (pancake model) has little impact on water production. The results are shown in Figure E17.

Figure E17 Water Production Sensitivity to Permeability

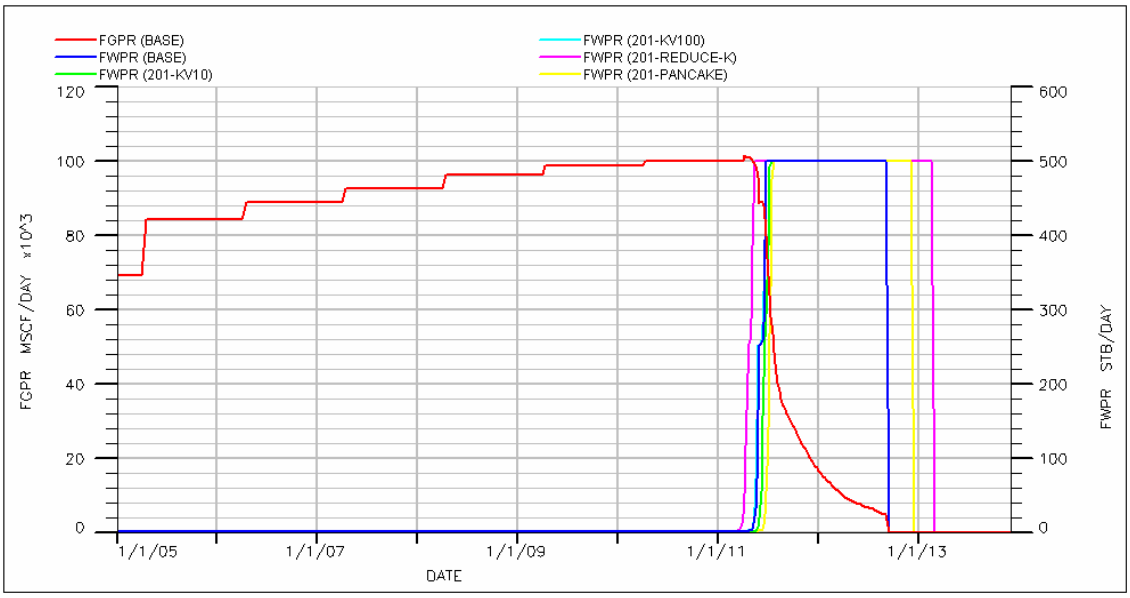

5.3.4 Sensitivity to Faults and Barriers

The sensitivity of the base case to faulting and barriers was investigated in the following cases:

- Sealing faults: 1 well @S-2 (Case 203-seal1)
- Sealing faults: 2 wells @S-2 & S-3 (Case 203-seal2)
- North lobe disconnected (Case 203-nonth)
- Sole-1 lobe disconnected (Case 203-nosth)
- North & Sole-1 lobes disconnected (Case 203-mainonly)

The results are shown in Table E11.

Table E11 Sensitivity to Faults and Barriers - Results

Case Summary	Case	GIP (Bcf)	Reserves (Bcf)	RF (%)
Base Case	base	346	227	66%
Sealing fault (1 well @S-2)	203-seal1	346	223	64%
Sealing fault (2 wells @S-2 & S-3)	203-seal2	346	227	66%
North lobe disconnected	203-nonth	346	225	65%
Sole-1 lobe disconnected	203-nosth	346	214	62%
North & Sole-1 lobes disconnected	203-mainonly	346	211	61%

Figure E18 shows recovery factor is relatively insensitive to whether or not the fault is sealing. Modelling suggests there is very little communication with the northern lobe. The base case sees 13.5 Bcf recovered from the Sole-1 lobe with wells in the main lobe. Therefore, no connection to the Sole-1 lobe results in lost reserves of ~13.5 Bcf. The impact of no communication to the north lobe is minimal.

Figure E18 Gas Production Sensitivity to Faults and Barriers

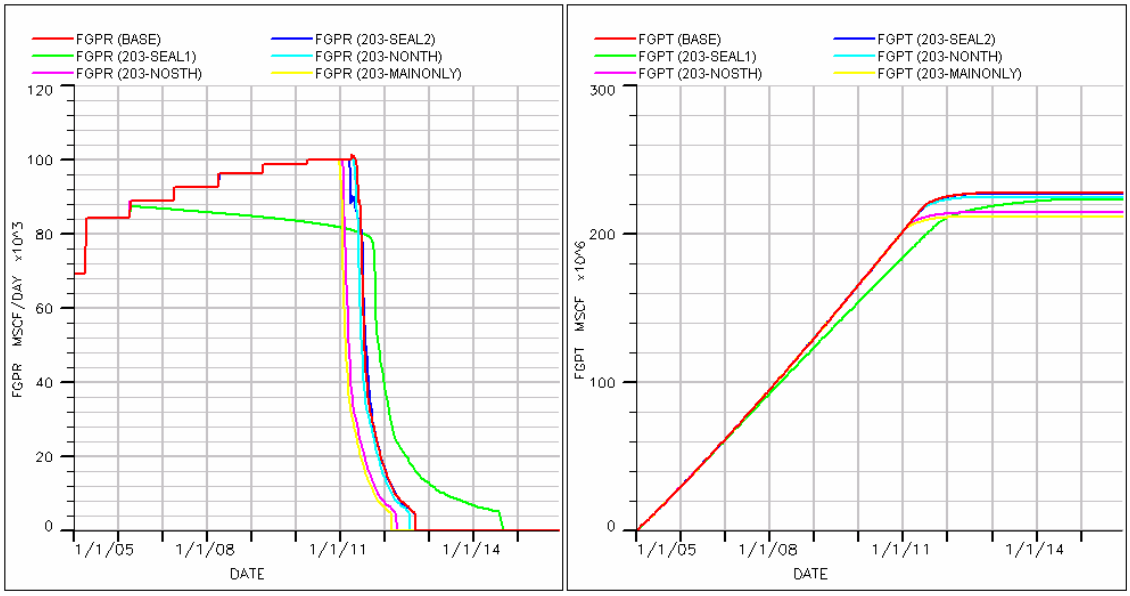

The impact of sealing faults only becomes evident when production occurs from one well instead of two. Production from one well results in a 6-month delay in the onset of water production. The impact of no communication with the north lobe has little impact but no communication with the Sole-1 lobe results in early breakthrough of water due to a reduction in accessible gas reserves but an unchanged gas production rate. The results are shown in Figure E19.

Figure E19 Water Production Sensitivity to Faults and Barriers

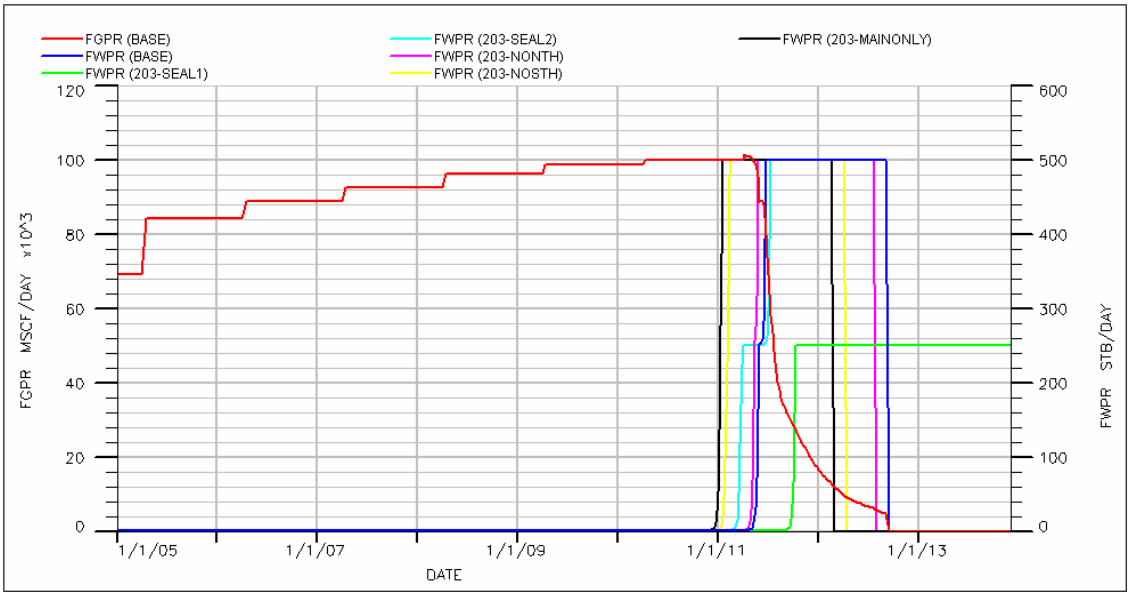

5.3.5 Sensitivity to Well Number (One Well Cases)

The performance of various one-well scenarios was investigated in the following cases:

- 1 well: vertical @S-2 – located at existing Sole-2 well location (Case 205-1vS2)
- 1 well: vertical @S-3 – crestal location in main lobe NW of Sole-2 (Case 205-1vS3)
- 1 well: vertical @S-4 – crestal location in north lobe (Case 205-1vS4)
- 1 well: horizontal @S-2 (Case 205-1hS2)

The results are shown in Table E12.

Table E12 Sensitivity to One Well - Results

Case Summary	Case	GIP (Bcf)	Reserves (Bcf)	RF (%)
Base Case	base	346	227	66%
1 well (vertical @S-2)	205-1vS2	346	224	65%
1 well (vertical @S-3)	205-1vS3	346	222	64%
1 well (vertical @S-4)	205-1vS4	346	26	7%
1 well (horizontal @S-2)	205-1hS2	346	225	65%

Figure E20 shows there is minimal difference between recovery from one or two wells in the main lobe. However with two wells it is possible to recover the gas quicker. There is little difference between Sole-2 and Sole-3 well locations and the only benefit of drilling a horizontal well is slight acceleration of reserves. A well in the north lobe is able to recover 26 Bcf, which is ~22 Bcf more than is recovered from wells in the main lobe, highlighting little communication between the north and main lobes.

Figure E20 Gas Production Sensitivity to One Well

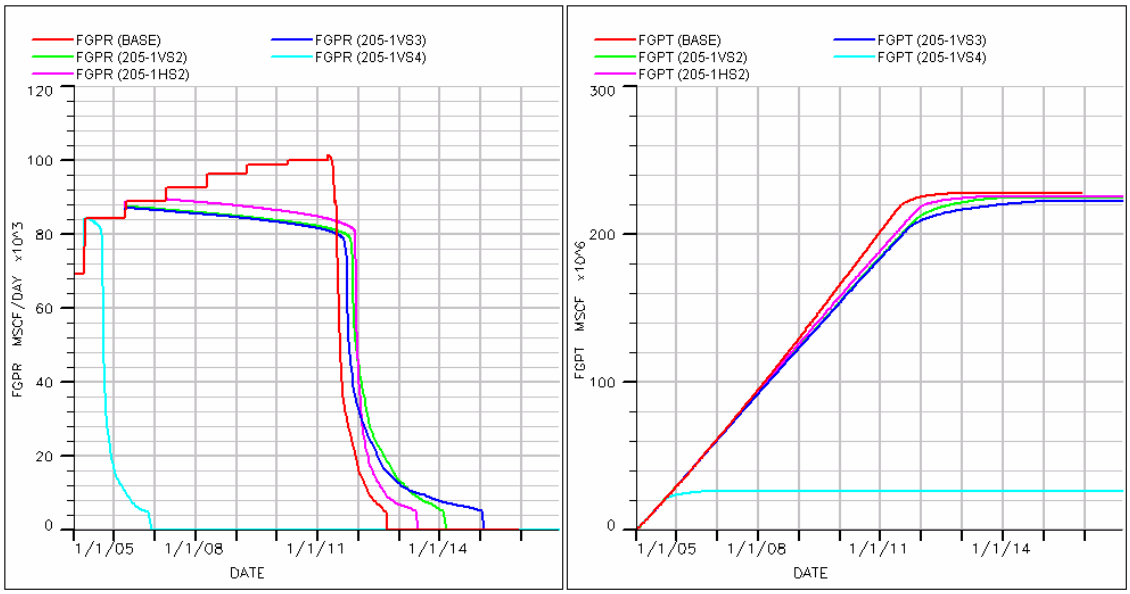

Figure E21 shows that placement of a single well will impact on the timing of water production. A well in the north lobe will result in water production within 9-months of first production. Modelling suggests that the proposed Sole-3 location will see water production 2 months earlier than the proposed Sole-2 location, and that a horizontal well at the Sole-2 location will see water production 2 months later than a vertical well at Sole-2.

Figure E21 Water Production Sensitivity to One Well

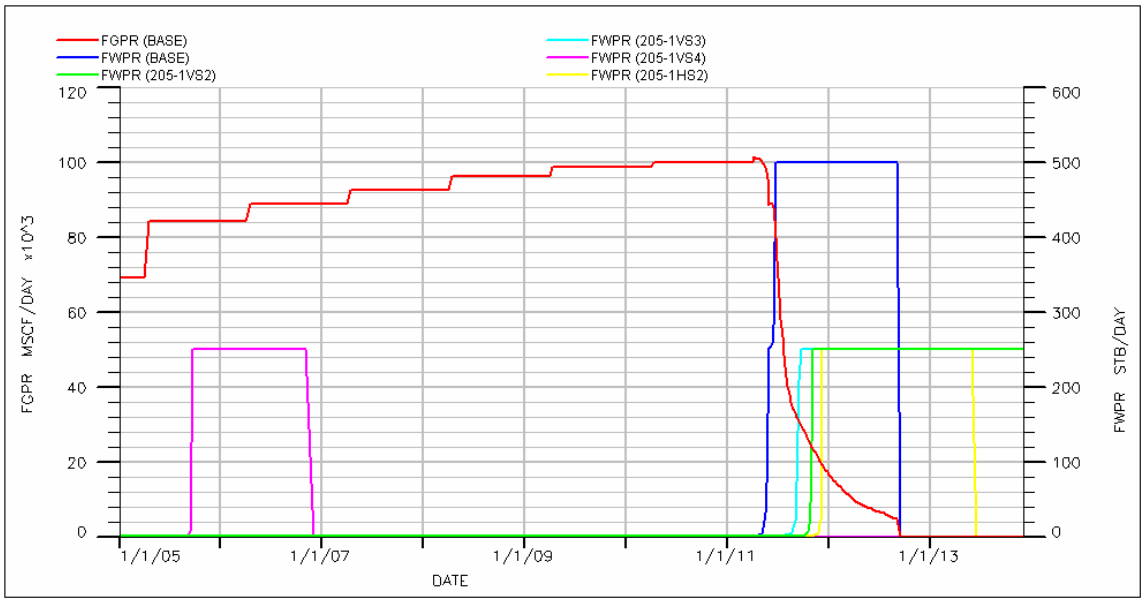

5.3.6 Sensitivity to Well Number (Two and Three Well Cases)

The performance of various two and three-well scenarios was investigated in the following cases:

- 2 well: horizontal @S-2, vertical @S-3 (Case 205-1h1v-S2S3)
- 2 well: horizontal @S-2, horizontal @S-3 (Case 205-2h-S2S3)
- 2 well: vertical @S-2 & S-4 - northern lobe (Case 205-2v-S2S4)
- 3 well: vertical @S-2, S-3 & S-4 - northern lobe (Case 205-3v-S2S3S4)

The results are shown in Table E13.

Table E13 Sensitivity to Two and Three Wells - Results

Case Summary	Case	GIP (Bcf)	Reserves (Bcf)	RF (%)
Base Case	base	346	227	66%
2 well (horizontal @S-2, vertical @S-3)	205-1h1v-S2S3	346	227	66%
2 well (horizontal @S-2, horizontal @S-3)	205-2h-S2S3	346	227	66%
2 well (vertical @S-2 & S-4 - north lobe)	205-2v-S2S4	346	247	71%
3 well (vertical @S-2, S-3 & S-4 - north lobe)	205-3v-S2S3S4	346	250	72%

Figure E22 shows that there is little difference in recovery whether wells in the main lobe are vertical or horizontal. There is also little benefit in terms of acceleration. However it is evident that drilling a well in the north lobe will increase recovery by ~20 Bcf. A well in the north lobe means reduced redundancy in the main lobe and potentially reduces available deliverability (as the north lobe has limited production capacity). Further optimisation work will need to be carried out on the benefits of this scenario. Gas marketing and economic analysis will determine which case is optimum.

Figure E22 Gas Production Sensitivity to Two and Three Wells

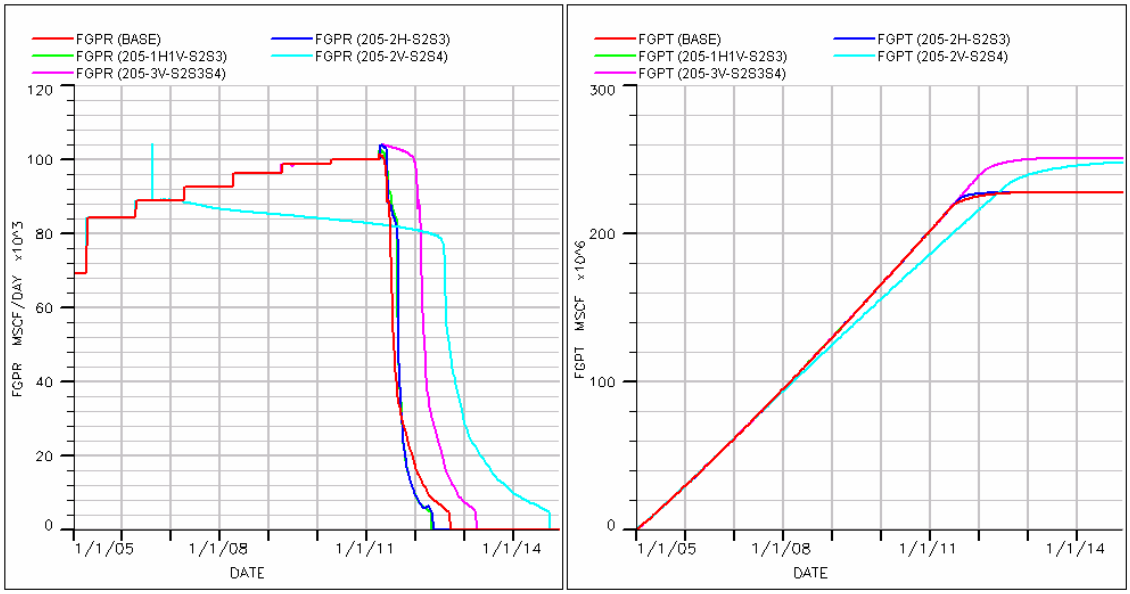

The impact of multiple wells suggests that placement is a major influence on the timing of water production. As seen in the one well cases, a well in the north lobe will result in water production significantly earlier than a well in the main lobe. The choice of vertical or horizontal wells has little influence on the start of water production but increasing the number of wells to three will delay water production. The results are shown in Figure E23.

Figure E23 Water Production Sensitivity to Two and Three Wells

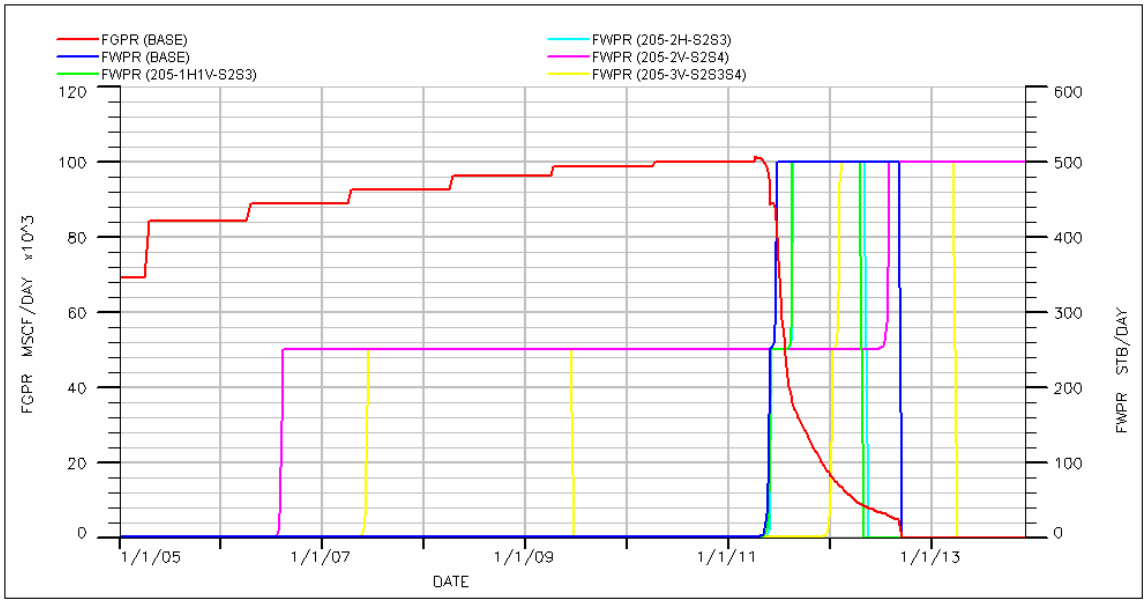

5.3.7 Sensitivity to Well Size, Pipeline Size and Plant Capacity

The sensitivity of the base case to well size, pipeline size and plant capacity was investigated in the following cases:

- Unconstrained - 1 well (5.5") & 14" pipeline (Case 204-15514)
- Unconstrained - 2 well (5.5") & 14" pipeline (Case 204-25514)
- Unconstrained - 1 well (7") & 14" pipeline (Case 204-17014)
- Unconstrained - 2 well (7") & 14" pipeline (Case 204-27014)
- Unconstrained - 2 well (7") & 16" pipeline (Case 204-27016)
- 85 MMscf/d plant capacity - 2 well (7") (Case 204-270120)

The results are shown in Table E14.

Table E14 Sensitivity to Well Size, Pipeline Size and Plant Capacity - Results

Case Summary	Case	GIP (Bcf)	Reserves (Bcf)	RF (%)
Base Case	base	346	227	66%
Unconstrained - 1 well (5.5") & 14" pipeline	204-1514	346	225	65%
Unconstrained - 2 well (5.5") & 14" pipeline	204-2514	346	227	66%
Unconstrained - 1 well (7") & 14" pipeline	204-1714	346	224	65%
Unconstrained - 2 well (7") & 14" pipeline	204-2714	346	227	65%
Unconstrained - 2 well (7") & 16" pipeline	204-2716	346	226	65%
85 MMscf/d plant capacity - 2 well (7")	204-pc85	346	228	66%

Figure E24 shows production rates have very little impact on reserves. The major benefit of increased production rate is acceleration of reserves.

Figure E24 ***Gas Production Sensitivity to Well Size, Pipeline Size and Plant Capacity***

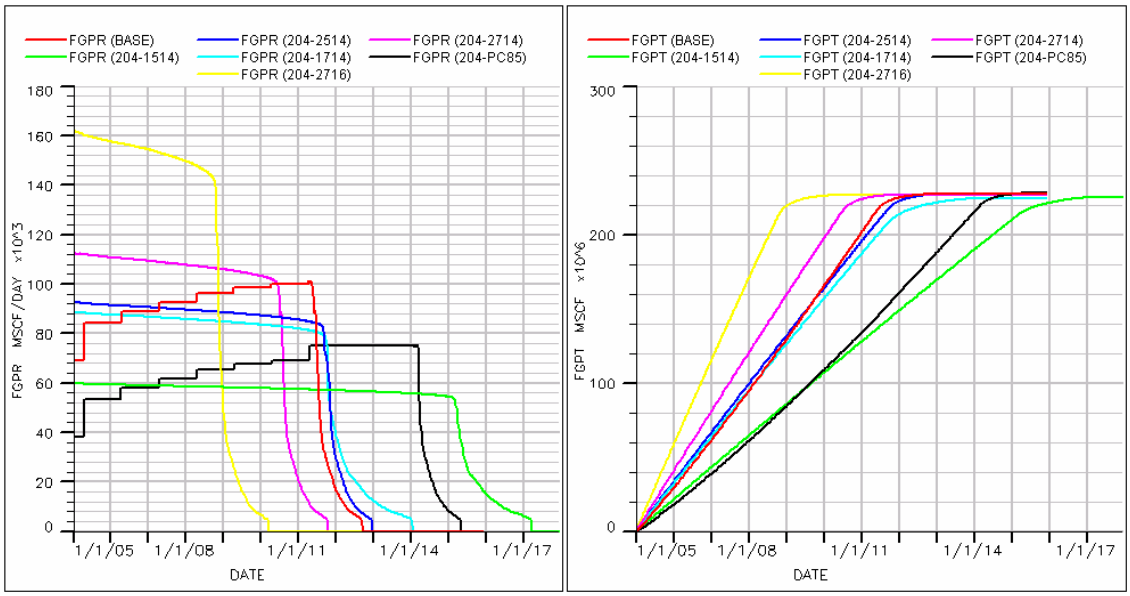

Figure E25 shows there is a delay in water production when only one well is drilled. However early breakthrough in water production occurs when pipeline size and plant capacity are increased. This is a result of depleting the Sole field at a higher rate than the base case scenario.

Figure E25 ***Water Production Sensitivity to Well Size, Pipeline Size and Plant Capacity***

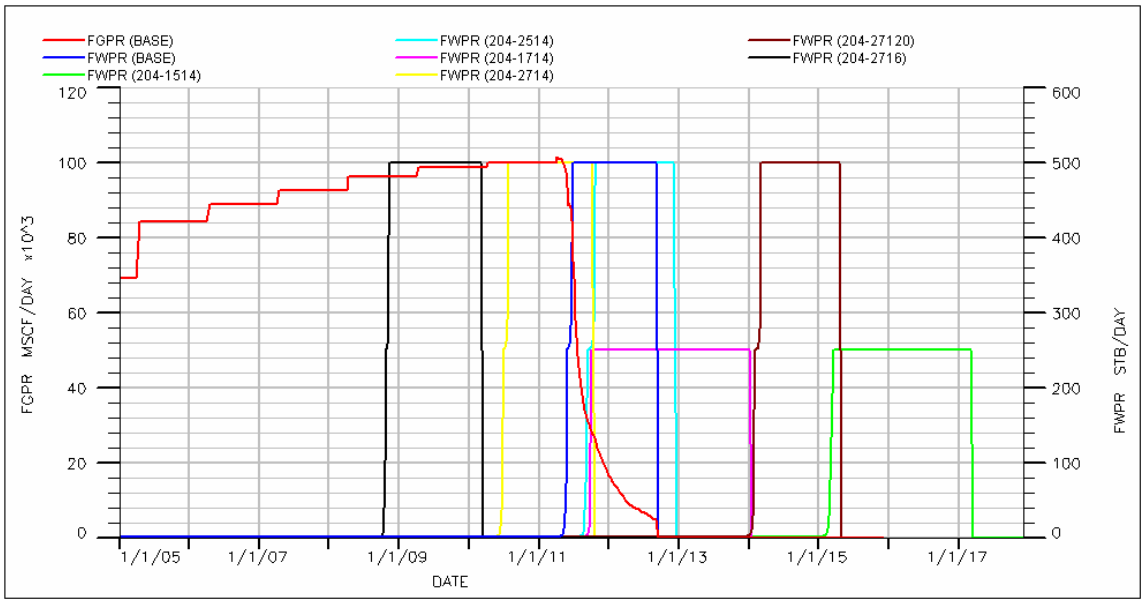

5.4 Local Grid Refinement

To more accurately predict the onset of water production and the likelihood of water coning, a radial grid refinement was applied to the grid blocks containing the two wells in the base case model. Grid blocks approximately 200m x 200m x 2m were refined to contain 10 radial divisions, 4 angular segments and a doubling of the number of grid blocks in the z-direction. As a result, one global grid block was refined to contain 80 local grid blocks. This refinement was applied to the grid blocks containing the wells, and was continued into the water zone at each well location. The local grid refinement at Sole-2 can be seen in Figure E26.

Figure E26 Local Grid Refinement at Sole-2

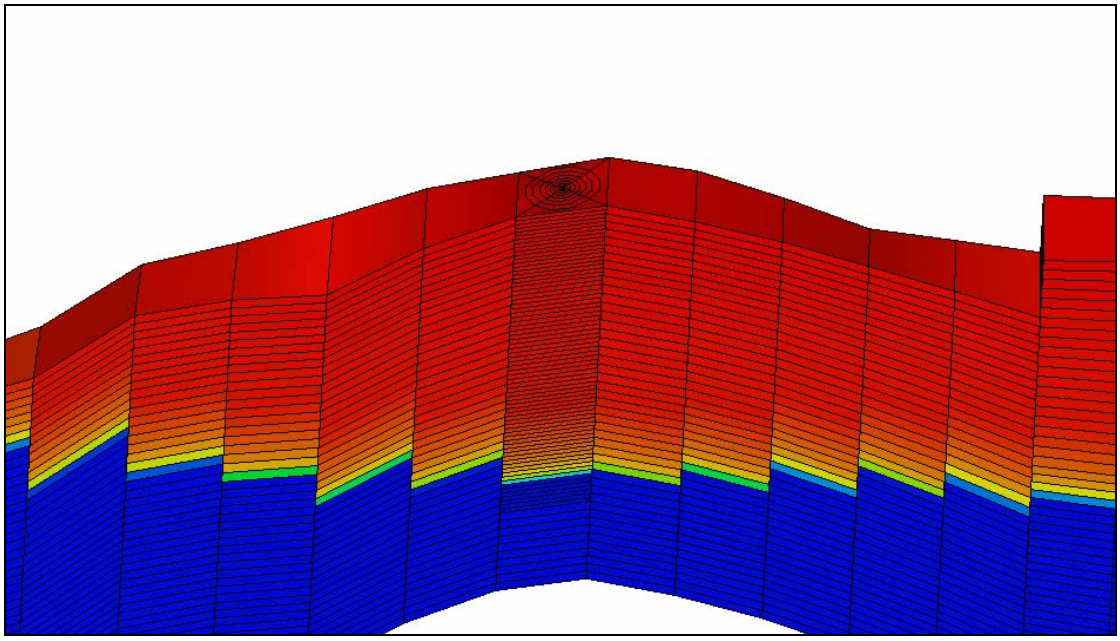

The sensitivity of the base case to local grid refinement was investigated in the following case:

- Base case with radial grid refinement at well (@S-2 & S-3) (Case radial)

The results are shown in Table E15.

Table E15 Sensitivity to Local Grid Refinement

Case Summary	Case	GIP (Bcf)	Reserves (Bcf)	RF (%)
Base Case	base	346	227	66%
Base Case (radial grid refinement @S-2 & S-3)	radial	346	227	66%

The refined grid has minimal impact on gas rate, total recovery and water production. Figure E27 shows water production commences one month earlier than the current base case prediction but total gas and water production is unchanged. The results also suggest water coning is not a concern in the two development wells, due to the minimal drawdowns expected and the high permeability of the reservoir.

Figure E27 Base Case and Local Grid Refinement Profiles

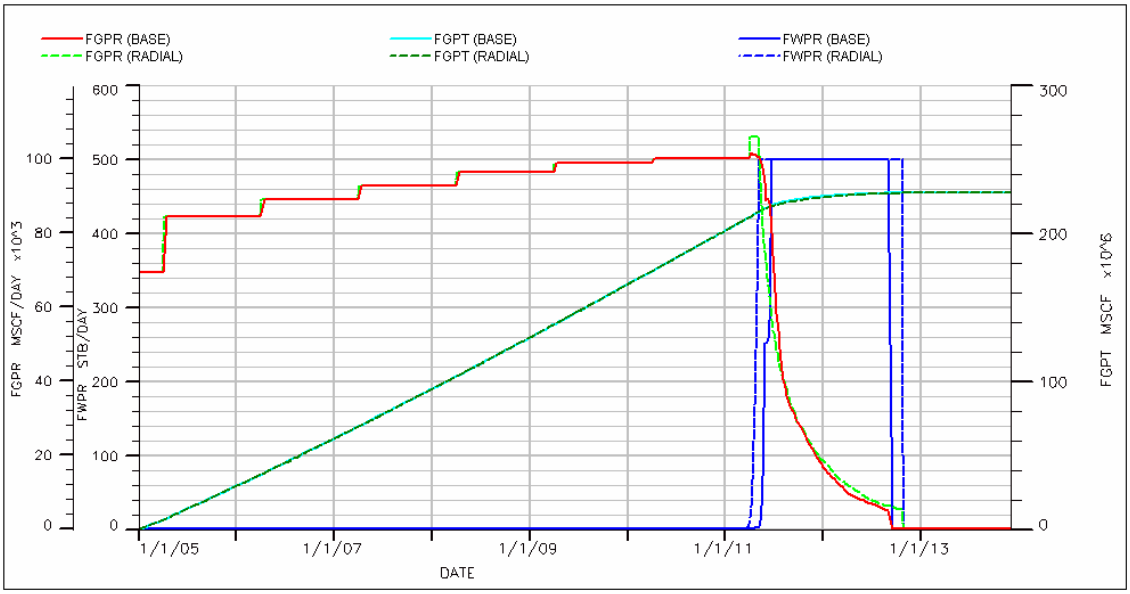

Figure E28 shows the change in gas saturation over time in the Sole-3 region for the local grid refinement case and gives an indication of the uniform nature of the water movement in a vertical direction. The results highlight that the best way to delay water production and maximize gas recovery is to complete the wells as high as possible in the gas zone.

Figure E28 Gas Saturation at Sole-3 region (t=0, 7yrs & end of life)

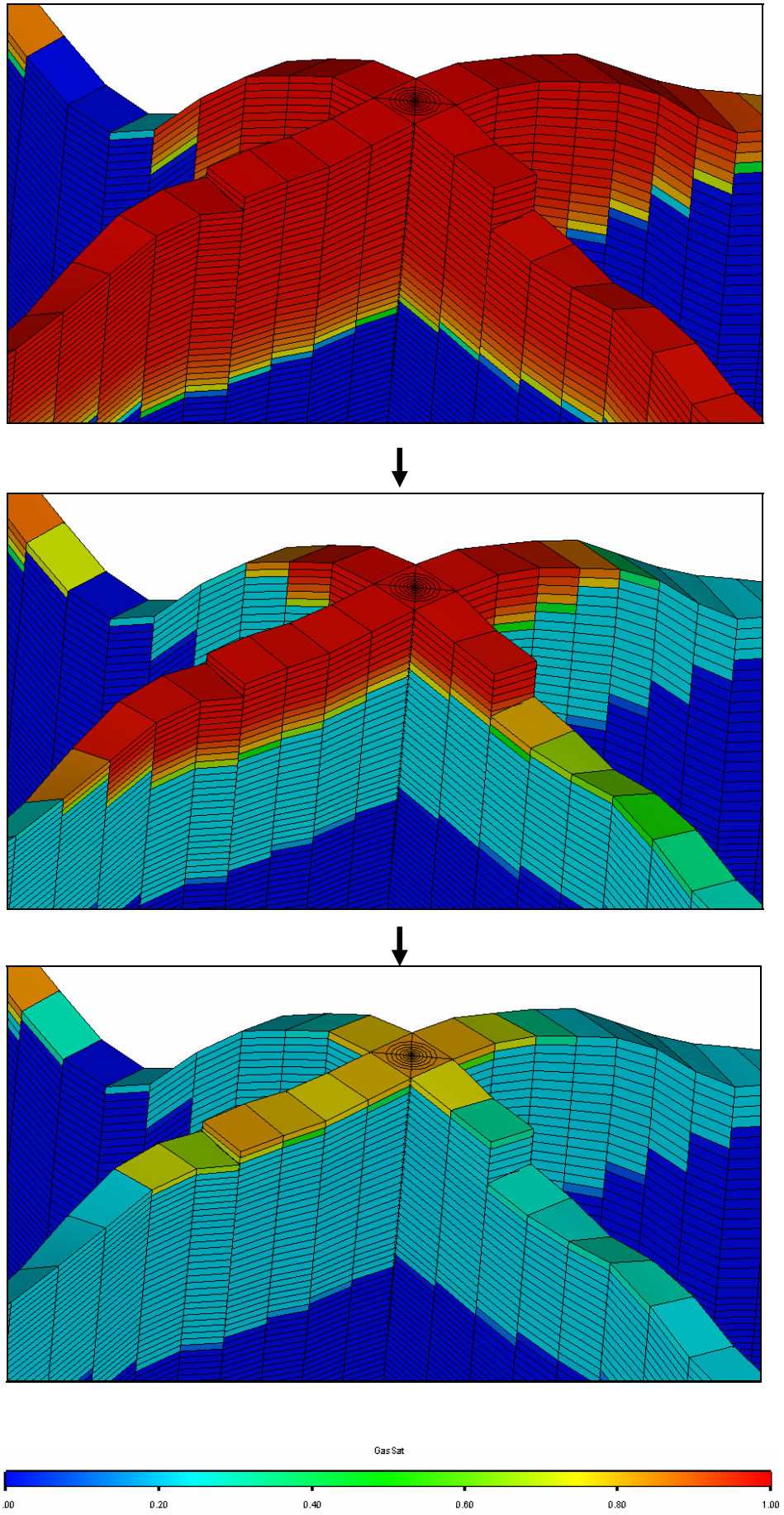

5.5 P90 and P10 GIP Models

Simulation models were also developed for the P90 and P10 GIP models. These models were based on a:

- P90 GIP model (GIP = 300 Bcf), based on the minimum case structural map (P90)
- P10 GIP model (GIP = 398 Bcf), based on the maximum case structural map (P10)

The results are shown in Table E16.

Table E16 P90 and P10 GIP Models - Results

Case Summary	Case	GIP (Bcf)	Reserves (Bcf)	RF (%)
P90 GIP	P90	300	199	66%
Base Case	base	346	227	66%
P10 GIP	P10	398	260	65%

GIP numbers were based on Probabilistic GIP values (Part A). The GIP from the upscaled minimum case structural map (P90) was approximately 6% higher than the Probabilistic P90 GIP. As a result a porosity (pore volume) multiplier was used to match the simulation model GIP with the Probabilistic P90 GIP. For the upscaled maximum case structural map (P10), the GIP was approximately 13% lower than the Probabilistic P10 GIP. The numbers were subsequently matched using an increase in Net-to-Gross (NTG) and porosity. In comparison, the GIP from the upscaled most likely (P50) structural map was 5% lower than the probabilistic P50 GIP and therefore an appropriate porosity multiplier was used to match the GIP numbers. The resulting porosity and NTG values for the simulation models were within the expected parameter distributions outlined in Part A.

Multipliers could also have been applied to the B_g value or gas saturation values. It was decided not to change the PVT data in order to keep consistent fluid properties across the model. Saturation height functions were also unchanged as saturation functions are linked to the relative permeability data in the simulation model and therefore would have required an additional change to the relative permeability functions.

It should be noted that the reserves numbers determined for the P10 and P90 GIP models differ from the Probabilistic Reserves numbers as the probabilistic reserves also consider the upside and downside recovery factor and Bg numbers. As a result, P90 reserves from probabilistic methods will be lower than the number determined in simulation, while the P10 probabilistic number will be higher.

A comparison of deterministic reserves (from simulation) and probabilistic numbers is as follows:

- The P90 GIP reserves of 199 Bcf (from simulation) corresponds to P84 on the probabilistic reserves distribution
- The P50 GIP reserves of 227 Bcf (from simulation) corresponds to P53 on the probabilistic reserves distribution
- The P10 GIP reserves of 260 Bcf (from simulation) corresponds to P17 on the probabilistic reserves distribution

Figure E29 shows the production rates and total production for the various models.

Figure E29 P90 and P10 GIP Models - Production Performance

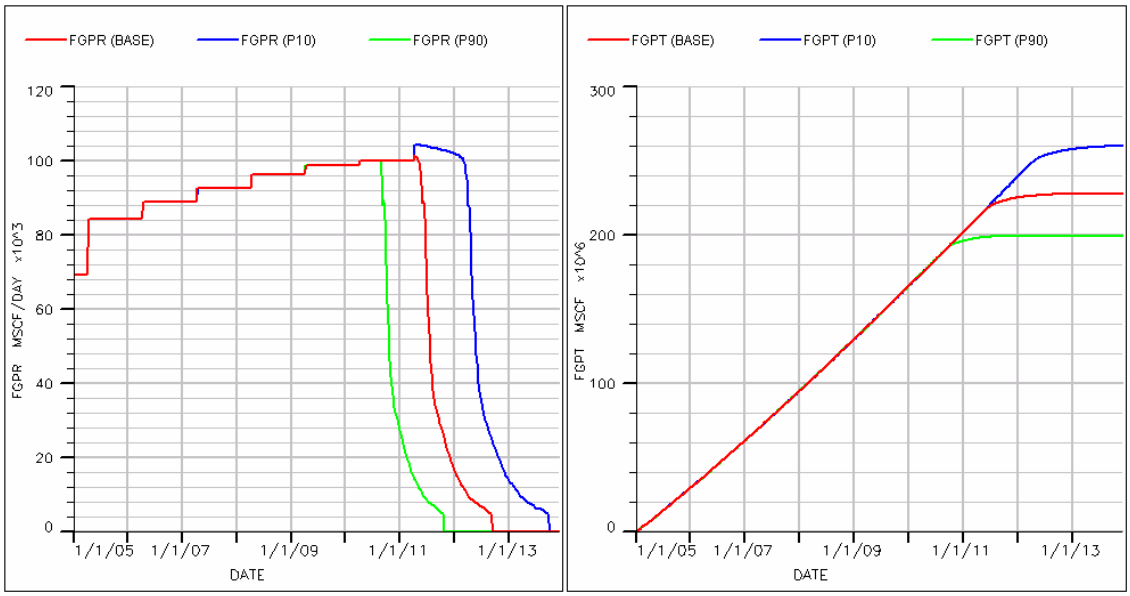

5.5.1 P90 & P10 Sensitivities

Sensitivities for residual gas and aquifer strength were found to have the largest impact on recovery in the base case model. As a result, these sensitivities were also carried out on the P90 and P10 models. The results are shown in Table E17 and Figure E30. A summary of the P10 and P90 sensitivities is included in Appendix EC.

Table E17 Sensitivity to Residual Gas & Aquifer Strength (P90 & P10 GIP models)

Case Summary	Case	GIP (Bcf)	Reserves (Bcf)	RF (%)
P90 - GIP = 300 Bcf				
Base Case (2 vertical wells)	P90	300	199	66%
Residual gas saturation = 10%	P90-sg10	300	231	77%
Residual gas saturation = 15%	P90-sg15	300	215	72%
Residual gas saturation = 25%	P90-sg25	300	183	61%
Aquifer: low perm. (100 md) & no bottom-drive	P90-a100	300	204	68%
Aquifer: high perm. (3000 md)	P90-a3000	300	199	66%
Aquifer: no aquifer	P90-noaq	300	223	74%
P10 - GIP = 398 Bcf				
Base Case (2 vertical wells)	P10	398	260	65%
Residual gas saturation = 10%	P10-sg10	398	304	76%
Residual gas saturation = 15%	P10-sg15	398	282	71%
Residual gas saturation = 25%	P10-sg25	398	238	60%
Aquifer: low perm. (100 md) & no bottom-drive	P10-a100	398	268	67%
Aquifer: high perm. (3000 md)	P10-a3000	398	258	65%
Aquifer: no aquifer	P10-noaq	398	292	73%

Figure E30 Reserves vs. Sgr and Aquifer Strength for P90, P50 and P10 GIP

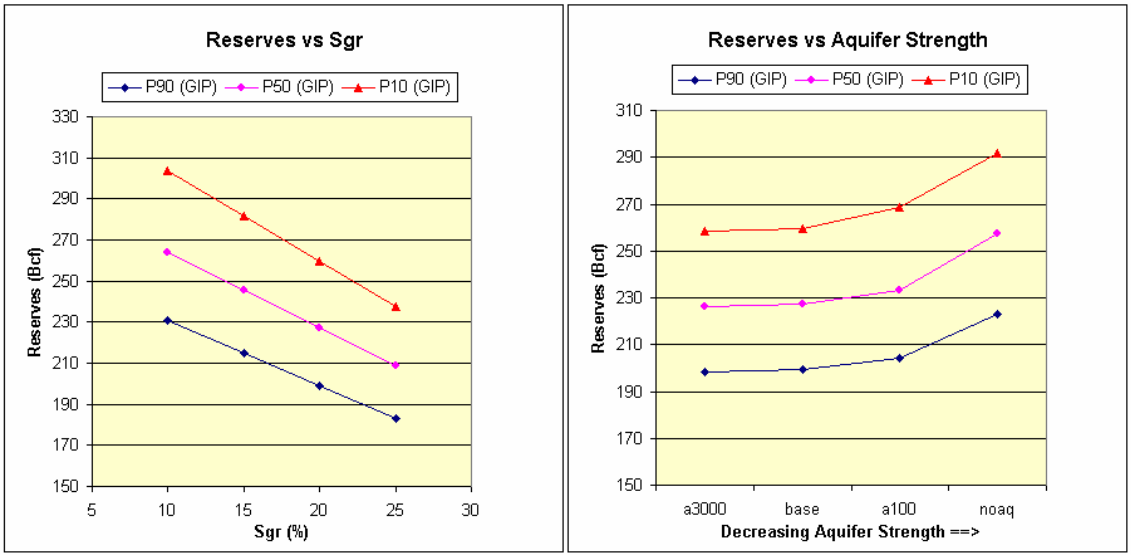

Figure E31 and Figure E32 show the sensitivity of the P90 and P10 GIP models to Residual Gas and Aquifer Strength. In summary, similar recovery factors are achieved to the P50 GIP model.

Figure E31 P90 sensitivities - Production Performance

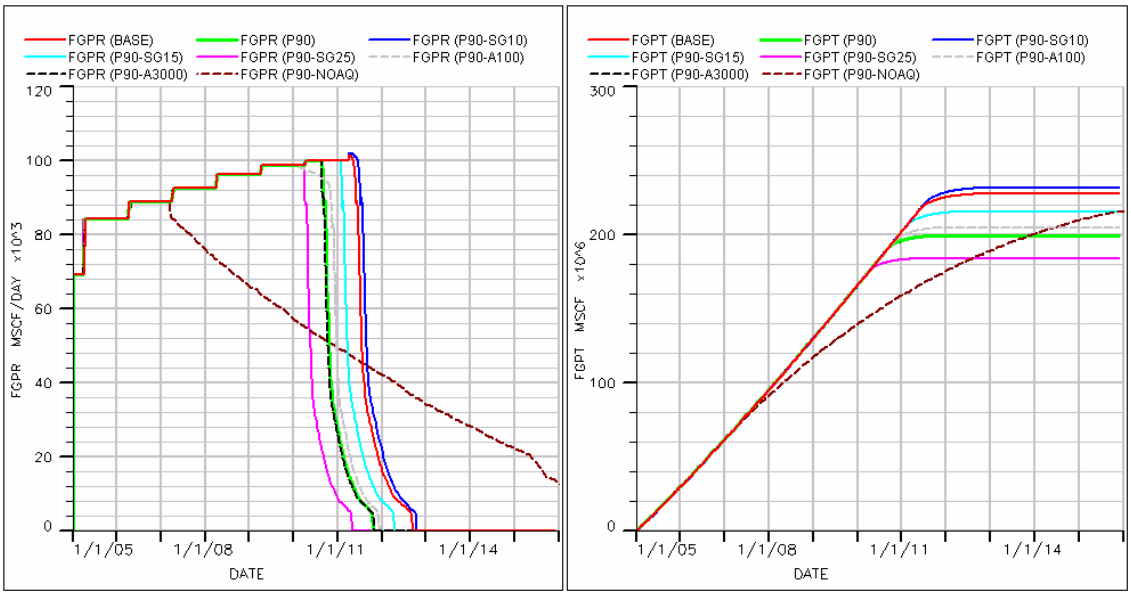

Figure E32 P10 sensitivities - Production Performance

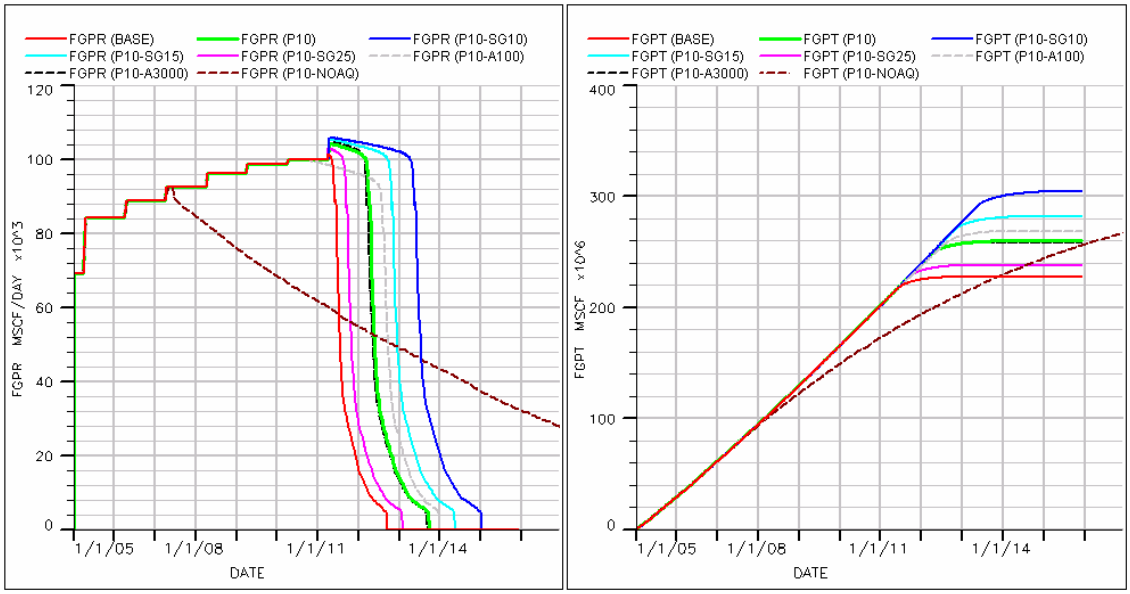

The impact on water production as a result of P90 and P50 GIP has a similar impact to residual gas, in that a reduction in recoverable gas volume but an unchanged gas production rate results in earlier water breakthrough. The results are shown in Figure E33.

Figure E33 Water Production Sensitivity to P90 and P10 GIP Models

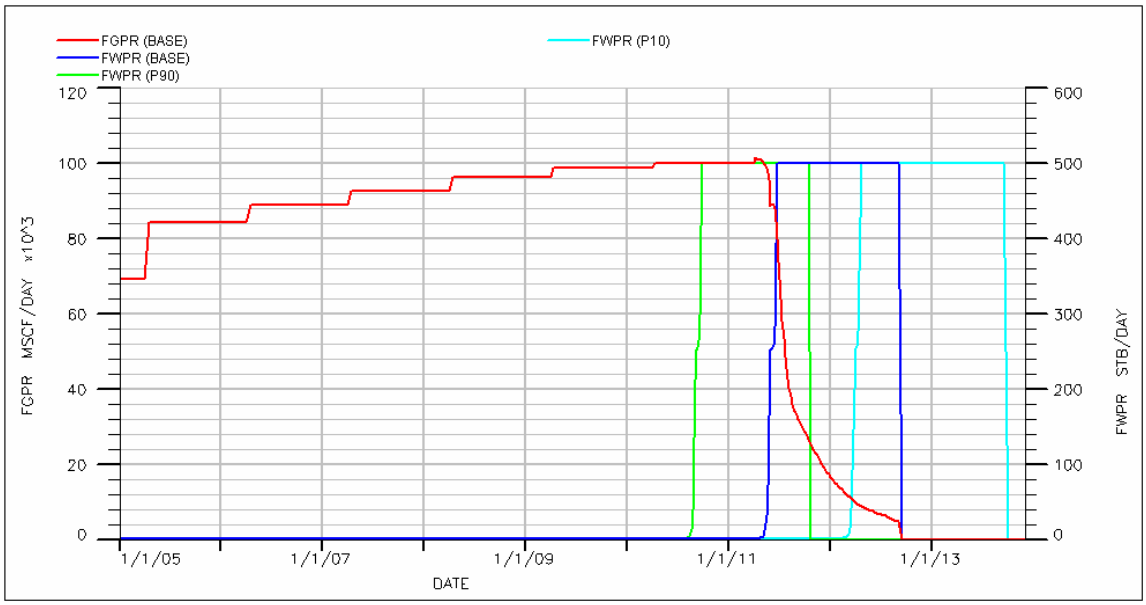

6 RESERVOIR MANAGEMENT

6.1 Overview

The Sole Field will be developed through 2 subsea wells in 'daisy chain' design with a 65km pipeline (14") linked to the PB onshore plant through a HDD shore crossing. The subsea wells will be controlled from the PB plant site, using a new ~65km long umbilical, run parallel with the pipeline. The selected subsea development concept and the subsequent well and facilities design will be based on a non-well intervention philosophy.

The development plan will evolve over the life of the project as reservoir data is collected primarily through production history and surveillance activities. Following field start-up, routine data acquisition will be restricted to onshore measurements and remote measurements of pressure/temperature at the subsea wellheads. During production life, data will be collected at regular intervals and be used as input to a history-matched dynamic simulation model. Updating of the model in this way will ensure that the prevailing description can be tested against field information to highlight any production impairment or to define and exploit the reserves upside.

The prime areas of production impairment risk are sand and water production. To minimise the risk to the facilities and plant early detection of these and other potential problems will be carried out at the wellhead. Wellhead pressures, temperature and flowrates will be measured on each well. The installation of sand and corrosion probes at the wellhead is planned. Permanent downhole gauges are not required.

6.2 Well Testing & Production Allocation

The proposed development wells will be flow-tested with completion in place prior to the commencement of production. This will establish an important baseline in terms of initial reservoir pressure and well productivity.

Initially, it is expected that both wells will operate on wellhead choke control, with control from the onshore plant. Additional flow regulation will be available using an onshore valve upstream of the plant. In the event of sub-critical flow at the chokes, flow measurement will be calculated from a formula derived from an equation of state for a non ideal gas and Bernoulli's theorem. However, during critical flow standard choke equations will be used to confirm production rates.

Total production will be measured onshore using fiscal meters. Production allocation to the wells will be achieved by choke equations. Each day, the total fiscal production measured onshore will be compared to the total well production estimated by means of the choke equations, to obtain an allocation factor. The allocated production per well will be the product of the allocation factor and the well production estimated using the choke equation. Given the dry nature of the gas, choke equations will provide a reliable means to estimate flow from each well.

As water production is not expected until late in the life of the field (excluding minor water production from water of condensation), the pressure drop across the choke will allow the well flowrate to be estimated to within a few percent by means of a choke equation. It is planned to calibrate the choke equation by flowing wells individually to shore during start-up. Thereafter, if well conditions change significantly and the allocation factor shows significant variation, it may be desirable to re-test individual wells to recalibrate the choke equation. If reliable allocated data cannot be generated using choke equations, wells may be tested by shutting in one well and individually measuring the flow from the other well onshore.

6.3 Pressure Measurement

Wellhead flowing pressure and temperature data will be continuously measured at the subsea manifold and transmitted to the onshore plant on a daily basis. Initially the wells will operate on wellhead choke control, with control from the onshore plant. Choke control at the wellheads will enable control of individual wells and allow balancing of production from the wells to manage depletion across the field.

Consideration was given during project design to the installation of permanent downhole gauges to monitor bottom hole flowing pressures. Given the accuracy with which bottomhole pressure can be derived from wellhead pressure using dry gas correlations, the additional cost of installing such gauges was not justified. Downhole pressure measurements are planned during clean up of both production wells, with the data to be used to tune tubing correlations for network modelling.

Plant arrival pressure will also be continuously monitored and this data will be used to tune the performance of the network model through calibration of the selected flow correlations.

6.4 Production Logging

Future well intervention for production logging is not planned. Consideration will only be given to obtaining additional downhole data, such as production logs, if well deliverability deviates significantly from prediction and if the remaining reserves justify the cost of diagnostic activities.

6.5 Reservoir Performance

The primary means of assessing reservoir performance in the short term will be individual material balance models tied into a network model that enables an estimation of hydraulic losses between each wellhead to the inlet valve of the onshore plant. The network model will be tuned with actual data on a regular basis. The material balance models will also be tuned regularly to investigate field behaviour and evaluate aquifer response.

In addition to material balance modelling, the reservoir simulation model will be utilised to track long-term reservoir performance during project life. Flow performance curves will be incorporated to allow the whole system to be modelled back to the onshore plant. It is anticipated that the existing geological/simulation models will be rebuilt after 6-12 months of production once early production trends have been established, in order to provide sufficient data for history matching.

Some modifications to the reservoir model may be required as a result of drilling information obtained from the development wells. The simulation model will be used to evaluate potential infill drilling locations, if required. In addition, the model will be used as a predictive tool to estimate ultimate recovery and provide estimates of the benefit of well interventions, if required.

6.6 Water Production

Early detection of water breakthrough will be carried out at the wellhead, based on the expected changes to pressure and temperature with water production. Produced water will be monitored by flowmeters on lines from the inlet separator. Production of gas and water will be controlled by chokes. Water production will be limited to 500 bwpd, in line with the planned water handling capacity of the onshore plant. Produced water will be stored in evaporation ponds, with provisions for further ponds or trucking offsite, if required.

APPENDIX EB – RUN SUMMARY OF P50 GIP MODELS

Case Summary	Case Name	Reserves (Bcf)	Field Life (years)	1st water (yrs)	RF (%)
Base Case	base	227.1	7.7	6.3	66%
Base Case with 5.5" wells	base5	226.9	8.1	6.8	66%
Residual gas saturation = 10%	201-sg10	263.7	8.8	7.3	76%
Residual gas saturation = 15%	201-sg15	245.3	8.2	6.8	71%
Residual gas saturation = 25%	201-sg25	208.9	7.1	5.8	60%
Aquifer: low perm. (100 md) & no bottom-drive	202-a100	233.4	7.8	6.6	67%
Aquifer: high perm. (3000 md)	202-a3000	226.3	7.6	6.3	65%
Aquifer: no aquifer	202-noaq	257.3	17.3	-	74%
kv/kh = 10%	201-kv10	227.2	7.7	6.4	66%
kv/kh = 100%	201-kv100	227.1	7.7	6.3	66%
Permeability reduced by 50% across model	201-reduce-k	224.9	8.1	6.2	65%
Constant properties (pancake model) - S-2 well	201-pancake	230.6	7.9	6.4	67%
Sealing fault (1 well @S-2)	203-seal1	222.9	9.6	6.7	64%
Sealing fault (2 wells @S-2 & S-3)	203-seal2	226.7	7.7	6.2	66%
North lobe disconnected	203-nonth	224.5	7.5	6.2	65%
Sole-1 lobe disconnected	203-nosth	213.9	7.3	6.0	62%
North & Sole-1 lobes disconnected	203-mainonly	211.1	7.1	5.9	61%
1 well (vertical @S-2)	205-1vS2	224.4	9.1	6.8	65%
1 well (vertical @S-3)	205-1vS3	222.1	10.0	6.6	64%
1 well (vertical @S-4)	205-1vS4	25.9	11.8	0.7	7%
1 well (horizontal @S-2)	205-1hS2	224.8	8.4	6.9	65%
2 well (horizontal @S-2, vertical @S-3)	205-1h1v-S2S3	227.2	7.3	6.3	66%
2 well (horizontal @S-2, horizontal @S-3)	205-2h-S2S3	227.3	7.3	6.3	66%
2 well (vertical @S-2 & S-4 - north lobe)	205-2v-S2S4	247.3	9.7	1.6	71%
3 well (vertical @S-2, S-3 & S-4 - north lobe)	205-3v-S2S3S4	250.1	8.2	2.3	72%
Unconstrained - 1 well (5.5") & 14" pipeline	204-1514	225.2	12.2	10.1	65%
Unconstrained - 2 well (5.5") & 14" pipeline	204-2514	226.8	7.9	6.6	66%
Unconstrained - 1 well (7") & 14" pipeline	204-1714	224.4	9.0	6.7	65%
Unconstrained - 2 well (7") & 14" pipeline	204-2714	226.6	6.8	5.4	65%
Unconstrained - 2 well (7") & 16" pipeline	204-2716	226.3	5.2	3.8	65%
85 MMscf/d plant capacity - 2 well (7")	204-pc85	227.8	10.3	9.0	66%
Base Case (radial grid refinement @S-2 & S-3)	Radial	227.0	7.8	6.2	66%

Notes:
GIIP = 346 Bcf, NTG = 95%, kv/kh = 75%, Plant inlet = 300psi, 500 bwpd limitation, Qmin = 5 mmscf/d
Base Case: 120 MMscf/d plant throughput (includes Patricia Baleen)
Sole production @ 97% availability & 90% remaining capacity
Base Case assumes 7" tubing for wells and 14" pipeline to shore
1St Water is defined as time when water production exceeds 10 bbls/day.

APPENDIX EC – RUN SUMMARY OF P90 & P10 GIP MODELS

P90 - GIP = 300 Bcf

Case Summary	Case Name	Reserves (Bcf)	Field Life (years)	1st water (yrs)	RF (%)
Base Case (2 vertical wells)	P90	199.2	6.8	5.6	66%
Residual gas saturation = 10%	P90-sg10	231.1	7.8	6.5	77%
Residual gas saturation = 15%	P90-sg15	215.0	7.3	6.0	72%
Residual gas saturation = 25%	P90-sg25	183.3	6.2	5.2	61%
Aquifer: low perm. (100 md) & no bottom-drive	P90-a100	204.4	6.9	5.8	68%
Aquifer: high perm. (3000 md)	P90-a3000	198.5	6.8	5.6	66%
Aquifer: no aquifer	P90-noaq	223.3	13.4	-	74%

P10 - GIP = 398 Bcf

Case Summary	Case Name	Reserves (Bcf)	Field Life (years)	1st water (yrs)	RF (%)
Base Case (2 vertical wells)	P10	259.5	8.7	7.2	65%
Residual gas saturation = 10%	P10-sg10	303.9	10.0	8.3	76%
Residual gas saturation = 15%	P10-sg15	281.5	9.3	7.7	71%
Residual gas saturation = 25%	P10-sg25	237.8	8.0	6.6	60%
Aquifer: low perm. (100 md) & no bottom-drive	P10-a100	268.4	8.9	7.6	67%
Aquifer: high perm. (3000 md)	P10-a3000	258.4	8.7	7.2	65%
Aquifer: no aquifer	P10-noaq	291.6	15.8	-	73%